WRC RESEARCH REPORT NO. 22

HYDRAULIC RESISTANCE IN ALLUVIAL CHANNELS

Ben Chie Yen
Assistant Professor

and

Ying-Chang Liou
Research Assistant
Department of Civil Engineering
University of Illinois

FINAL REPORT

Project No. A-033-ILL

July 1, 1968 - June 30, 1969

The work upon which this publication is based was supported by funds provided by the U.S. Department of the Interior as authorized under the Water Resources Research Act of 1964, P.L. 88-379
Agreement No. 14-01-0001-1632

UNIVERSITY OF ILLINOIS
WATER RESOURCES CENTER
3220 Civil Engineering Building
Urbana, Illinois 61801

July 1969

ABSTRACT

HYDRAULIC RESISTANCE IN ALLUVIAL CHANNELS

An analytical study was conducted for the determination of the Weisbach resistance coefficient for flow in sand-bed straight channels. Available experimental data were reanalyzed based on dimensional analysis and fluid mechanics concepts. It was found that for flows having width to depth ratio greater than 5, there is a unique and systematic relationship among the Weisbach resistance coefficient f, the Froude number of the flow, and the sediment particle size to hydraulic radius ratio. The bed form which also is a dependent variable is also uniquely determined. For flow with Froude number less than 0.5 where its effect can be neglected, the resistance coefficient can be expressed as a function of the Reynolds number, sediment size to hydraulic radius ratio, and the sediment terminal fall velocity to shear velocity ratio. Application of the results for engineering purposes is also discussed. The technique for engineering applications of the results appear to be quite simple.

Yen, Ben Chie and Liou, Ying-Chang
HYDRAULIC RESISTANCE ALLUVIAL CHANNELS
Final Report to Office of Water Resources Research, Department of the Interior, July 1969, Washington, D.C., 66 p.
KEYWORDS--*alluvial channels/ dimensional analysis/ *flow resistance/ hydraulics/ open-channel flow/ *sediment

ACKNOWLEDGMENT

This report is based on the result of a research project carried out under the financial support provided by the Office of Water Resources Research, Department of the Interior through Water Resources Center of the University of Illinois, under grant Project No. A-033-ILL, Agreement No. 14-01-0001-1632. Thanks are due Dr. V. T. Chow, Professor of Hydraulic Engineering, Department of Civil Engineering, University of Illinois for his encouragement in carrying out this research. Cooperation from Dr. B. B. Ewing, Director of Water Resources Center, for matters related to the progress of the project is also appreciated. Last, but not the least, the authors wish to thank Mrs. Joanne Garth for her willingness and cooperation in typing the manuscript.

TABLE OF CONTENTS

LIST OF FIGURES

NOTATION

B = width of channel

D = hydraulic mean depth of flow

d_s = mean size of sediment particles

$\vec{F}$ = body force of fluid

$\vec{F}_B$ = body force of sediment

$\vec{F}_R$ = resistance force on sediment by fluid

$\mathbb{F}$ = Froude number, $V/\sqrt{gD}$

F_i = function, $i = 1,2, \cdots$

f = Weisbach resistance coefficient

g = gravitational acceleration

k = measure of surface roughness for rigid boundary

$\vec{M}$ = angular momentum

m_s = mass of sediment particle

N = dimensionless flow or channel nonuniformity parameter

p = pressure intensity

Q = discharge

R = hydraulic radius

$\mathbb{R}$ = Reynolds number, $4\rho VR/\mu$

S = water surface slope

$\vec{T}$ = torque

t = time

V = mean velocity of flow

$\vec{V}_s$ = velocity vector of sediment particle

V_t = terminal fall velocity of sediment particle

V_τ = shear velocity, $\sqrt{\tau_o/\rho}$

ζ = dimensionless cross-sectional shape factor

μ = dynamic viscosity of fluid

ρ = density of fluid

ρ_s = density of sediment

σ = standard deviation from mean size or gradation of sediment

τ_o = average bed-shear stress

I. INTRODUCTION

The economy and effectiveness of many water resources projects related to flow in channels depend on the accuracy of the determination of hydraulic resistance. The resistance to flow affects not only the capacity and stage of an alluvial channel but also the velocity distribution and the configuration of the movable bed. Thus, the hydraulic resistance is a vital factor in successful design and planning of fluvial hydraulic engineering works such as flood control, river channel training, bank stabilization, sediment and erosion control, canal design, and pollutant diffusion control in rivers.

The flow resistance of clear water in a fixed-bed straight channel has been studied extensively. For the case of steady uniform flow it can be predicted with a satisfactory degree of certainty. However, in alluvial streams the problem is complicated by the presence of sediment in the flow. Observations have shown (46)* that the friction factor for sediment-laden flows varies over an appreciable range. The conventional engineering practice of using the Manning or Chezy resistance factors in predicting alluvial channel flow behaviors has been found, in many instances, to be unsatisfactory. No rigorous theoretical method has been developed to predict satisfactorily the hydraulic resistance of sediment-laden flows because of the complexity of the problem. Most of the analytical approaches on the subject considering the flow and sediment characteristics actually deal with bed

---

*Numerals in parentheses refer to corresponding items in REFERENCES.

configuration instead of dealing explicitly with the hydraulic resistance. The present study is an attempt to relate the hydraulic resistance to sediment and flow characteristics by analyzing available experimental data based on dimensional analysis and fluid mechanics concepts. The main objectives are to investigate the relative importance of the factors affecting hydraulic resistance and to develop a simple technique to determine the hydraulic resistance, without advanced knowledge of bed form of the flow, for engineering applications.

II. RELATED PREVIOUS WORK ON FLOW IN MOVABLE-BED CHANNELS

Since Gilbert (17) observed and recorded different types of bed form in flow with fine particles, the effect of sediment on resistance to flow has been given serious consideration by many investigators. The majority of previous investigations may be categorized into a group focusing on the sediment transport capacity and transport process of sediment-bearing flows. Most of the studies in this category were based on results of laboratory flume experiments. Available data together with associated experimental conditions prior to 1942 were compiled by Johnson (21). Among the numerous investigations in this catagory the representative works after 1942 are those by Einstein (11, 12), Vanoni (45), Kalinski (22), Bagnold (2), Barton and Lin (4), Brooks (8), Laursen (29), Yalin (49), Colby (10), and Stein (44). In these studies the flow resistance is related to either the sediment transport capacity or the boundary shear stress.

Chien (9), Vanoni and Brooks (46), Liu and Hwang (32), Kennedy (24), Simons and Richardson (40, 42), Engelund (14), Raudkivi (35), and Smith (43), each gave excellent discussions on the subject of resistance to sediment-bearing flows. However, none of the above mentioned studies offers a simple direct technique to evaluate the hydraulic resistance in movable-bed channels.

Kennedy (23, 25), Langbein (27), Liu (31), Simons (39), Simons and Richardson (41), Vanoni and Nomicos (48), and others investigated the mechanics of formation of bed form and the effects of bed form on hydraulic resistance. Their primary emphasis was on the influences of bed shear

and Froude number on different types of bed form. In this approach the estimation of hydraulic resistance is impossible without advanced knowledge of the bed form for the flow.

Meyer-Peter and Muller (34), Einstein and Barbarossa (13), and Shen (38) using the concept of superposition subdivided the total resistance, expressed as a shear, into components. Despite the fact that this approach appears to be quite promising, further verification of the linear assumption of superposition for the complex problem is necessary. Moreover, in this approach the effect of sediment on the flow is not obvious and explicit expressions for the relationship between the sediment characteristics and the flow resistance have not been obtained. Recently following this concept of subdivision Vanoni and Hwang (47) succeeded in relating friction factors to geometric parameters of sand ripples, and Raudkivi (36) attempts to corelate the bed shear to the friction factor.

Certain investigators including Lacey (26), Blench (5, 6), Ackers (1), Garde and Ranga Raju (15, 16), and Haynie and Simons (19) studied the problem from the regime theory approach. Others, such as Leopold and Maddock (30) and Langbein (28), using field observations, studied the problem from the physiographic point of view.

III. DIMENSIONAL ANALYSIS AND THEORETICAL BACKGROUND

For a fluid carrying cohesionless sediment flowing in a straight channel, the hydraulic resistance to the flow is a function of the flow characteristics, the geometry of the channel cross section, and the properties of the fluid and sediment. For steady flow the Weisbach resistance coefficient f can be expressed as

$$f = F_1(\rho, \mu, \rho_s, d_s, \sigma, g, S, V, D, \zeta) \tag{1}$$

where ρ and μ are density and dynamic viscosity of the fluid; ρ_s, d_s, and σ are density, mean size, and gradation or standard deviation from the mean size of the sediment particles, respectively; g is gravitational acceleration; S is average surface slope; V and D are mean velocity and hydraulic mean depth of the flow, respectively; and ζ represents a nondimensional cross-sectional shape factor. In Eq. 1 the average surface slope S is assumed to be equal to the average channel bottom slope over the length of the channel considered. It is also assumed that, except for the irregularities of the bed formation, channel cross-sectional nonuniformities such as contraction and expansion do not exist. Otherwise factors describing the nonuniformities should be included.

Through dimensional analysis, Eq. 1 can be written nondimensionally as

$$f = F_2\left(\mathbb{F}, \mathbb{R}, \frac{d_s}{R}, \sigma, \frac{\rho_s}{\rho}, S, \zeta\right) \tag{2}$$

where the Froude number of the flow, $\mathbb{F} = V/\sqrt{gD}$, represents the effect of gravity on the flow; the Reynolds number, $\mathbb{R} = 4\rho VR/\mu$, represents the effect of viscosity of the fluid; and R is the hydraulic radius of the cross section. The dimensionless parameter d_s/R indicates the interference of the sediment particles, directly by their sizes or indirectly by formation of various types of bed forms, to the flow in the channel.

For natural rivers or laboratory experiments with sand and water, the ratio ρ_s/ρ is approximately a constant. Since the effect of gravity to the flow is accounted for by the Froude number, the term S in Eq. 2 indicates the additional pressure gradient on the sediment particles and its subsequent effect on the hydraulic resistance. Usually the magnitude of S is small and its effect on f is relatively less important. However, since the parameters ρ_s/ρ and S are two of the factors controlling the mobility of the sediment particles in the flow, these two parameters may be combined into one representing the relative mobility of the sediment. By introducing the shear velocity $V_\tau = \sqrt{\tau_o/\rho}$, where $\tau_o = \rho gRS$ is the average bed-shear stress, and the terminal fall velocity of the sediment V_t, Eq. 2 can be simplified as

$$f = F_3 \left(\mathbb{F}, \mathbb{R}, \frac{d_s}{R}, \sigma, \frac{V_t}{V_\tau}, \zeta\right) \tag{3}$$

For steady flow in channels without sediment, the expression for the Weisbach resistance coefficient, Eq. 3, may be simplified with the allowance of nonuniformity of the flow, as

$$f = F_4 (\mathbb{F}, \mathbb{R}, \frac{k}{R}, \zeta, N) \tag{4}$$

where k is a measure of the boundary roughness and N is a nondimensional parameter describing the nonuniformity. Rouse (37) suggested that steady open-channel flow resistance can be subdivided into three groups: (a) Surface resistance due to viscosity of the fluid and geometric texture of the channel boundary as represented by the parameters $\mathbb{R}$, k/R, and ζ in Eq. 4; (b) form resistance due to nonuniformity of the flow as represented by the dimensionless parameter N; and (c) wave resistance due to existence of a free surface in a gravity field, as represented by the Froude number in Eq. 4. Only for steady uniform flow with no sediment and no appreciable gravity effect have the Manning roughness factor and Chezy's coefficient been theoretically justified (51). At present no generally acceptable quantitative description of the effects of the Froude number and nonuniformity of the flow on hydraulic resistance has been developed.

The presence of sediment particles in the flow affects the hydraulic resistance in two distinct ways: (a) The channel boundary may be modified as a result of the formation of different types of bed forms such as dunes and ripples. The flow is locally nonuniform. Consequently the form resistance and wave resistance (due to the deformation of the free surface) would be modified. Even if the movement of the ripples, dunes, or antidunes is very slow, such bed forms would act somewhat similar to large roughness elements which produce additional energy losses (50), (b) The velocity gradient of the flow, in particular the local velocity gradient of the fluid around the moving sediment particles

is modified, and consequently, the processes of energy dissipation due to viscosity of the fluid is altered.

Theoretically, the motion of the fluid and sediment, and consequently the flow resistance, can be found by solving the equations of continuity and motion of the fluid

$$\nabla \cdot \vec{V} = 0 \tag{5}$$

$$\frac{\partial \vec{V}}{\partial t} + (\vec{V} \cdot \nabla)\ \vec{V} = \vec{F} - \frac{1}{\rho} \nabla p + \frac{\mu}{\rho} \nabla^2 \vec{V} \tag{6}$$

and the equations of motion for the sediment

$$m_s \frac{d\vec{V}_s}{dt} = \vec{F}_B - \vec{F}_R \tag{7}$$

$$\frac{d\vec{M}}{dt} = \vec{T} \tag{8}$$

where $\vec{V}$ is the velocity vector of the fluid, t is time, $\vec{F}$ is the body force of the fluid, p is pressure, and ρ and μ are the density and viscosity of the fluid, respectively, m_s is the mass of the sediment particle under consideration, $\vec{V}_s$ is the velocity vector of the sediment, $\vec{F}_B$ is the body force of the sediment particle, $\vec{F}_R$ is the resistance force on the sediment by the fluid, $\vec{T}$ is the torque acting on the sediment, and $\vec{M}$ is the angular momentum of the sediment. However, in practice even with known appropriate initial and boundary conditions usually numerical solutions of these equations cannot be obtained because of their highly

nonlinear nature and the present insufficient knowledge on turbulence. Therefore, experimental results are usually interpreted to yield the needed information.

In most of the laboratory experiments, the channel has a rectangular corss section so that the cross-sectional shape factor can be represented by B/D, where B is the width of the channel, and the sediment particles are of approximately uniform size. Hence, Eq. 3 may be simplified as

$$f = F_4 \left(\mathbb{F}, \mathbb{R}, \frac{d_s}{R}, \frac{V_t}{V_T}, \frac{B}{D}\right) \tag{9}$$

IV. ANALYSIS OF DATA

The dependence of the Weisbach resistance coefficient on six dimensionless control parameters as indicated in Eq. 3 necessitates a large amount of reliable data to be analyzed to yield useful information on hydraulic resistance in movable-bed channels. Because of the accuracy and reliability of the measurements, only those data obtained from controlled laboratory flume experiments are used in the present study. A summary of the laboratory experimental data used in the present study is listed in Table 1. Details on experimental equipment and conditions from which these data were obtained can be found in the respective original publications.

The data utilized were analyzed in accordance with Eq. 9. Since for all the data utilized the experiments were performed in flumes with rectangular cross sections, the channel width B is equal to the water surface width, and the average depth of the flow is equal to the hydraulic mean depth D. Consequently, the hydraulic radius R is computed as

$$R = \frac{BD}{B+2D} \tag{10}$$

and for a given discharge Q the mean velocity is

$$V = \frac{Q}{BD} \tag{11}$$

In addition, the following equations were used for the computation of the magnitude of the parameters in Eq. 9.

$$\mathbb{F} = \frac{V}{\sqrt{gD}} \tag{12}$$

$$\mathbb{R} = \frac{4\rho VR}{\mu} \tag{13}$$

$$V_\tau = \sqrt{gRS} \tag{14}$$

$$V_t = \frac{\rho g}{18\mu} \left(\frac{\rho_s}{\rho} - 1\right) d_s^2 \tag{15}$$

The data analyzed are tabulated in Appendix.

Although the limited amount of available laboratory experimental data with $B/D < 5$ had been analyzed, preliminary study revealed that these data were insufficient to yield significant information. Therefore, it was decided that experimental data with $B/D < 5$ would not be included in this report. However, in the tables in Appendix, for the series of experiments with B/D both greater and less than 5, the data for $B/D < 5$ were also included for the sake of completeness. Moreover, for certain experiments there were insufficient information to make side-wall corrections to account for the difference in surface roughness between channel bed and side walls. For the sake of consistency no side-wall correction was made in this study. Such side-wall correction is particularly important for flows with small B/D.

The analyzed results with $B/D > 5$ are present graphically in four figures. Figure 1 is a plot of f vs. $\mathbb{F}$ with the source of data

shown for each point. The bed forms for the points are also given, if the information is available from the original data. The value of d_s/R is shown at the lower right corner of each point and the value of the Reynolds number at upper left corner. Figure 2 is a similar plot of f vs. F as Fig. 1 for plane bed. For each point in Fig. 2 the values of V_t/V_τ and B/D as well as R and d_s/R are given. It should be noted that only for Fig. 2 analyzed data for flows with plane bed having $B/D < 5$ are included. Figure 3 is a logarithmic plot of f vs R in the same format as the Moody diagram for plane bed data. The corresponding f - R curves from the Moody diagram for steady uniform flows on rigid boundary with various values of relative surface roughness k/R are also shown for convenience in comparison. Figure 4 consists of logarithmic plots of f vs. R for $F < 0.45$ for three different ranges of V_t/V_τ. For each point in Fig. 4 the values shown are, from left to right, upper corners V_t/V_τ, B/D, lower corners F and d_s/R.

TABLE 1. Summary of Data Utilized

Source of Data	Flume Size			Grain Size		No. of Runs	Discharge		Slope		Depth		Mean Velocity		Reference
	ft			mm			cfs		%		ft		fps		
	Width	Depth	Length	Median Size	Gradation σ		min.	max.	min.	max.	min.	max.	min.	max.	
Colorado State University	8	2	150	0.19	1.30	40	0.96	22.33	0.0055	0.950	0.42	1.09	0.78	4.58	18
				0.27	1.56	20	5.11	21.84	0.0077	1.022	0.45	1.13	0.79	4.93	
				0.28	1.67	37	4.16	22.02	0.007	1.007	0.30	1.07	0.82	4.93	
				0.45	1.60	45	1.84	21.62	0.015	1.01	0.19	1.00	0.65	5.54	
				0.47	1.54	54	6.92	21.42	0.042	0.960	0.30	1.33	1.13	5.32	
				0.93	1.54	43	4.49	22.69	0.013	1.28	0.38	1.11	1.00	6.07	
Barton and Lin	4			0.18		31	0.90	9.10	0.044	0.210	0.300	1.38	0.71	3.60	4
Brooks	0.875	0.833	40	0.16	1.11	12	0.20	0.54	0.18	0.35	0.155	0.30	0.93	2.15	8,46
Vanoni and Brooks	2.79	1	60	0.137	1.38	16	0.51	3.84	0.039	0.280	0.203	0.553	0.77	2.53	8,46
Kennedy	0.875	0.833	40	0.549	1.14	16	0.20	0.78	0.55	2.72	0.074	0.346	1.65	4.65	23
				0.233	1.47	14	0.22	0.78	0.26	1.60	0.147	0.346	1.57	3.42	
Kennedy	2.79	1	60	0.233	1.47	13	0.68	3.33	0.32	2.29	0.145	0.356	1.35	3.45	23
Kennedy	2.79	1	60	0.142	1.38	9	1.05	1.40	0.056	0.25	0.228	0.550	0.91	2.21	24
Vanoni and Hwang	3.61		130	0.206	1.46	6	2.26	3.82	0.0642	0.130	0.578	0.603	1.05	1.83	47
Stein	4			0.4	1.50	51	1.80	17.0	0.1013	1.079	0.30	0.81	1.50	5.62	44

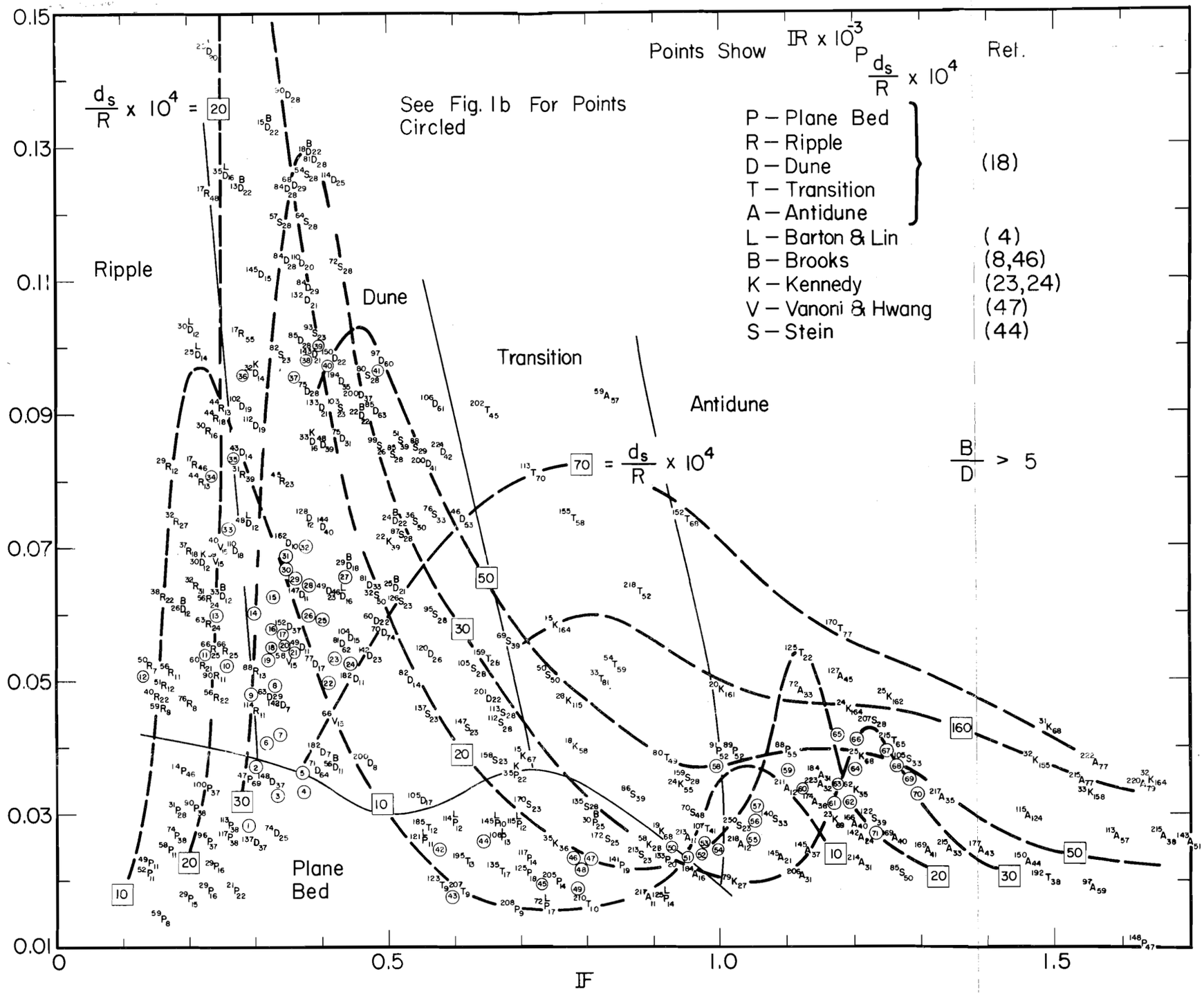

FIG. 1 (a) RESISTANCE COEFFICIENT AS FUNCTION OF FROUDE NUMBER

(1) $^{118}D_{38}$

(2) $^{45}P_{70}$, $^{51}P_{68}$

(3) $^{65}R_{30}$, $^{51}P_{69}$

(4) $^{59}P_{66}$

(5) $^{70}P_{60}$, $^{58}P_{70}$, $^{132}D_{8}$

(6) $^{122}D_{9}$, $^{60}D_{25}$

(7) $^{69}R_{30}$, $^{52}P_{70}$

(8) $^{122}D_{12}$

(9) $^{103}R_{12}$

(10) $^{108}D_{16}$, $^{106}R_{8}$

(11) $^{93}R_{8}$

(12) $^{47}R_{19}$

(13) $^{59}R_{22}$, $^{82}R_{11}$

(14) $^{66}D^{L}_{11}$, $^{63}D_{25}$

(15) $^{70}D_{28}$, $^{15}D^{B}_{11}$

(16) $^{53}V_{15}$

(17) $^{110}D_{13}$

(18) $^{63}D_{11}$, $^{36}D_{11}$

(19) $^{49}D^{L}_{13}$

(20) $^{55}D^{L}_{12}$, $^{56}V_{15}$

(21) $^{48}D^{B}_{12}$, $^{66}R_{18}$

(22) $^{65}D_{11}$, $^{169}D_{14}$

(23) $^{128}D_{13}$, $^{87}D_{16}$

(24) $^{33}D^{K}_{17}$, $^{96}D_{61}$, $^{74}D_{14}$

(25) $^{45}D^{L}_{15}$

(26) $^{127}D_{12}$, $^{110}D_{14}$

(27) $^{33}D^{K}_{17}$

(28) $^{91}D_{11}$, $^{72}D_{12}$

(29) $^{42}D_{40}$

(30) $^{68}D_{30}$

(31) $^{154}D_{10}$

(32) $^{33}D^{L}_{18}$

(33) $^{40}D^{B}_{12}$

(34) $^{31}R_{33}$

(35) $^{60}R_{26}$, $^{50}R_{14}$

(36) $^{33}D^{L}_{15}$

(37) $^{33}D^{L}_{18}$

(38) $^{85}D_{28}$

(39) $^{152}D_{21}$

(40) $^{76}D_{31}$

(41) $^{205}D_{37}$

(42) $^{109}P_{12}$, $^{92}P^{L}_{13}$

(43) $^{75}P^{B}_{12}$, $^{82}P^{B}_{11}$

(44) $^{188}T_{14}$, $^{135}P^{L}_{11}$

(45) $^{58}K_{27}$

(46) $^{35}P^{B}_{22}$, $^{35}P^{K}_{23}$

(47) $^{192}S_{23}$, $^{21}B_{25}$, $^{36}P^{K}_{24}$

(48) $^{187}P_{15}$

(49) $^{116}D^{L}_{14}$

(50) $^{192}S_{25}$

(51) $^{218}A_{11}$

(52) $^{49}K_{36}$

(53) $^{140}A_{21}$, $^{232}P_{29}$

(54) $^{236}S_{23}$

(55) $^{104}S_{39}$, $^{21}K_{70}$

(56) $^{176}S_{29}$, $^{213}A_{12}$

(57) $^{213}S_{25}$, $^{196}A_{17}$

(58) $^{158}A_{14}$, $^{56}K_{63}$

(59) $^{184}S_{28}$, $^{23}K_{67}$

(60) $^{157}A_{19}$

(61) $^{238}A_{32}$, $^{233}S_{26}$

(62) $^{153}S_{33}$, $^{225}A_{33}$

(63) $^{29}K_{57}$

(64) $^{232}A_{33}$, $^{171}A_{40}$

(65) $^{169}A_{18}$, $^{170}A_{19}$

(66) $^{161}A_{39}$

(67) $^{44}K_{45}$

(68) $^{30}K_{57}$

(69) $^{46}K_{116}$

(70) $^{184}P_{34}$, $^{141}A_{54}$

(71) $^{86}A_{55}$

Fig. 1 (b) Points circled in Fig. 1a.

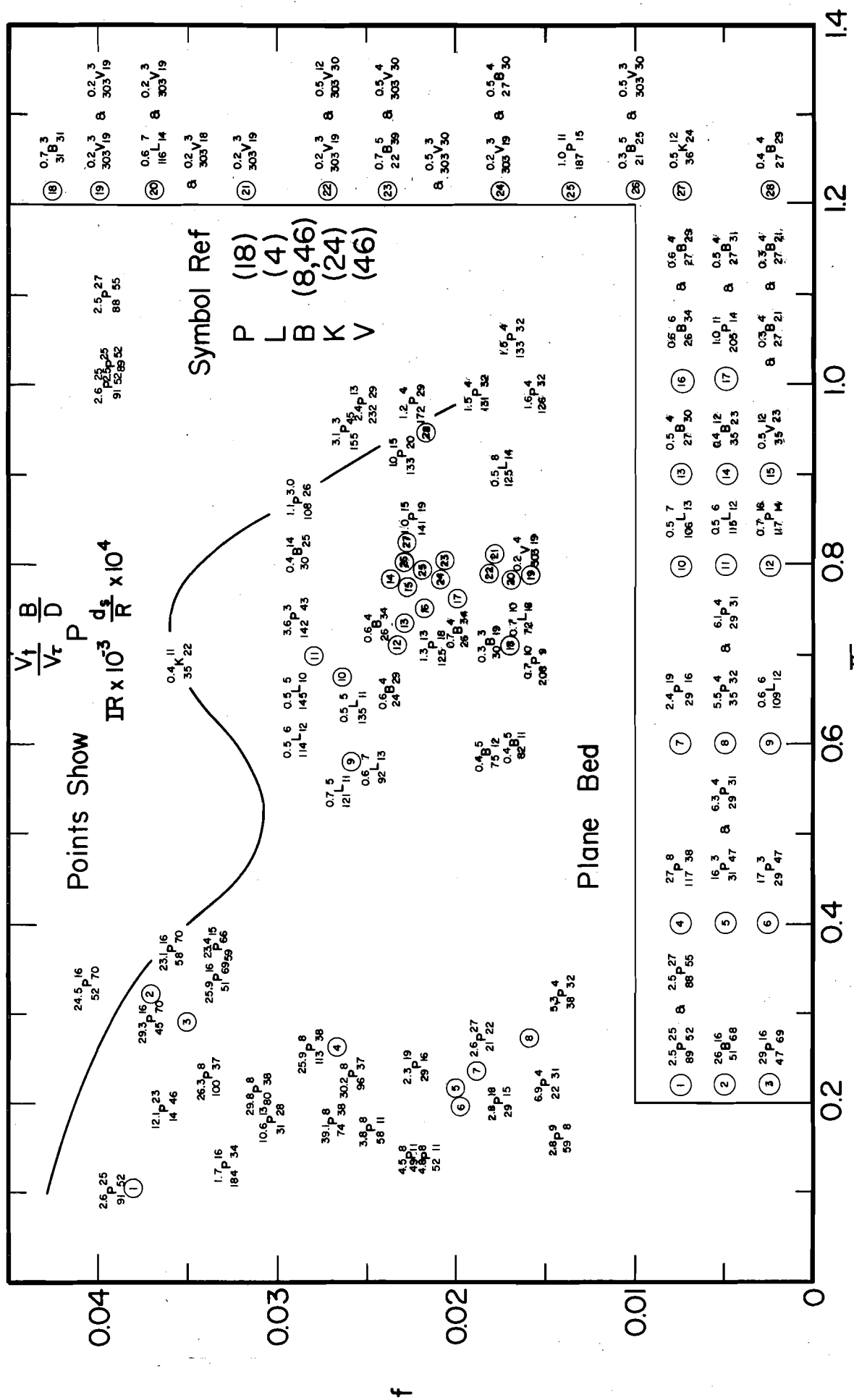

FIG. 2 PLANE BED REGION IN f – IF RELATIONSHIP

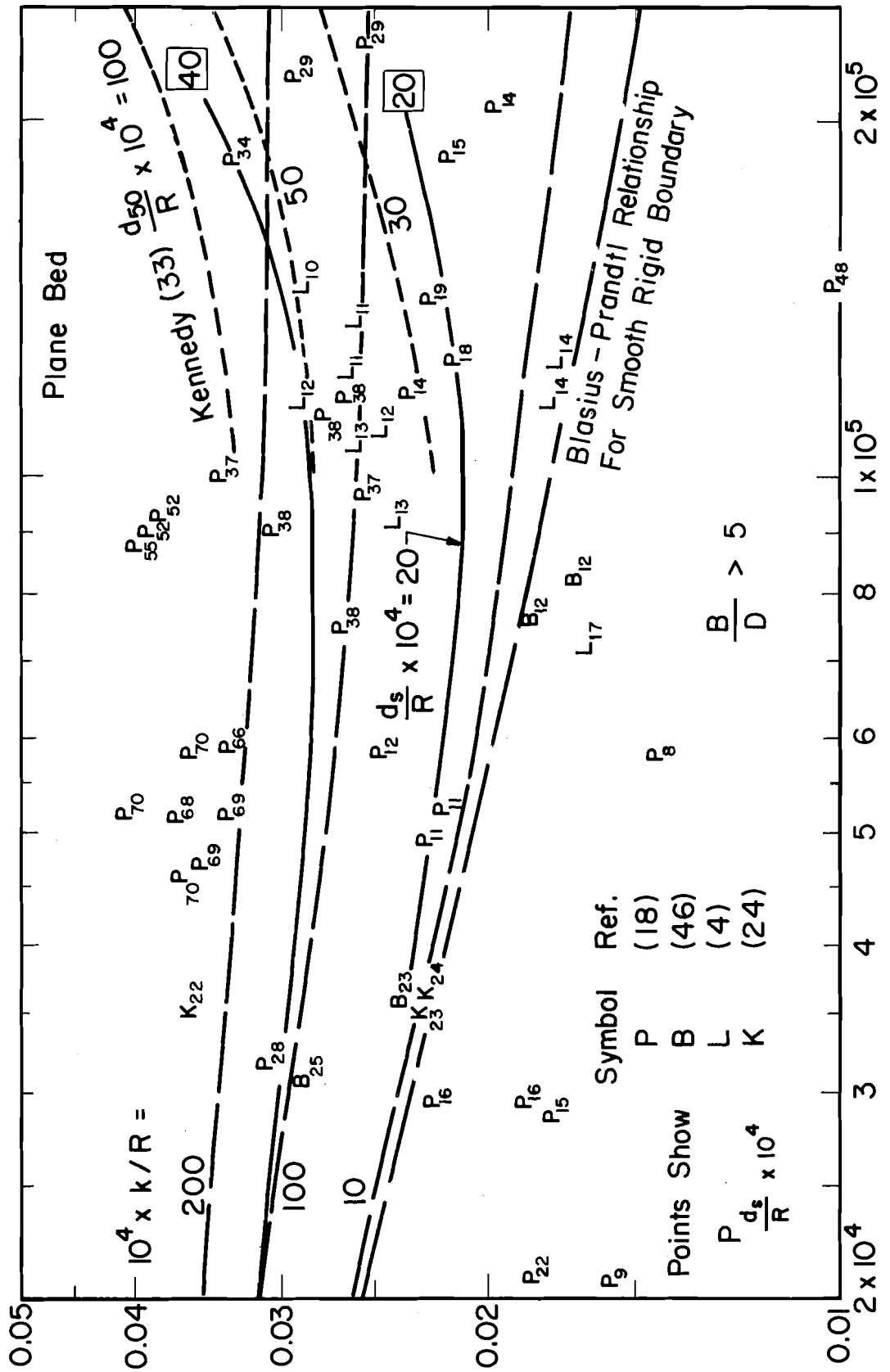

FIG. 3 RESISTANCE COEFFICIENT AS FUNCTION OF REYNOLDS NUMBER FOR PLANE BED

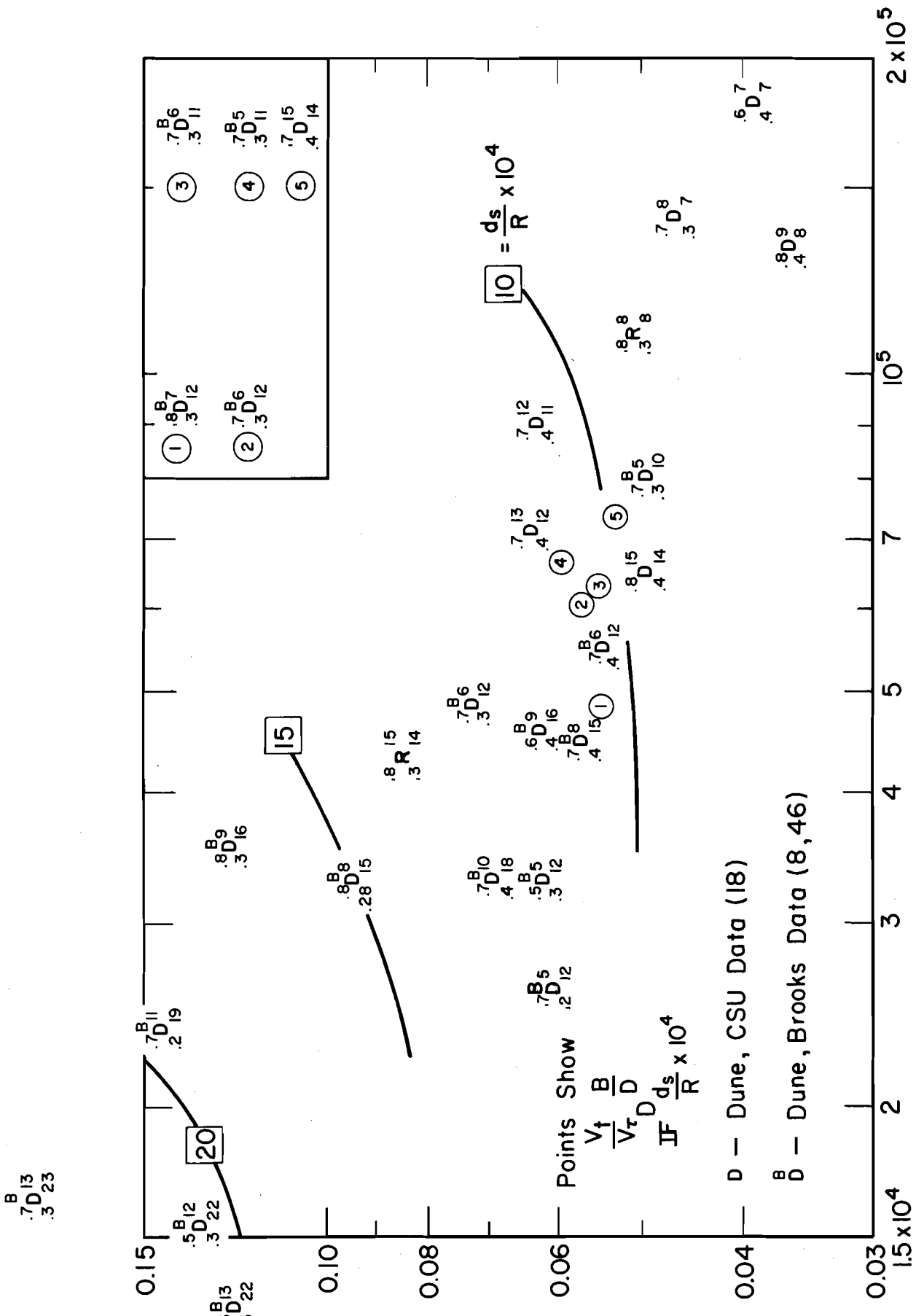

FIG. 4 RESISTANCE COEFFICIENT AS FUNCTION OF REYNOLDS NUMBER FOR B/D > 5, Fr < 0.45
(a) $V_t/V_\tau = 0.5 - 0.8$

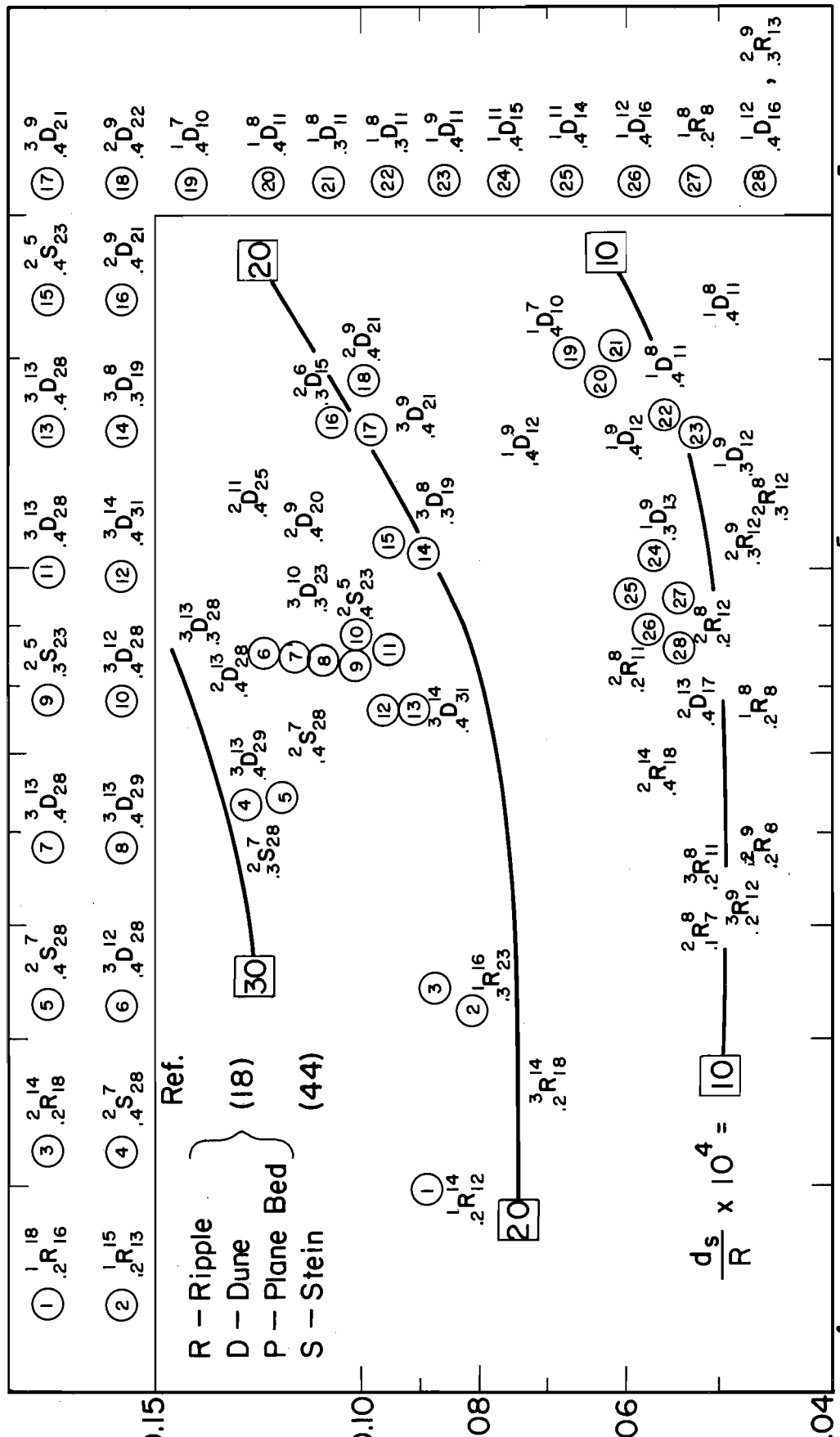

FIG. 4 (b) $V_t / V_\tau = 1-3$

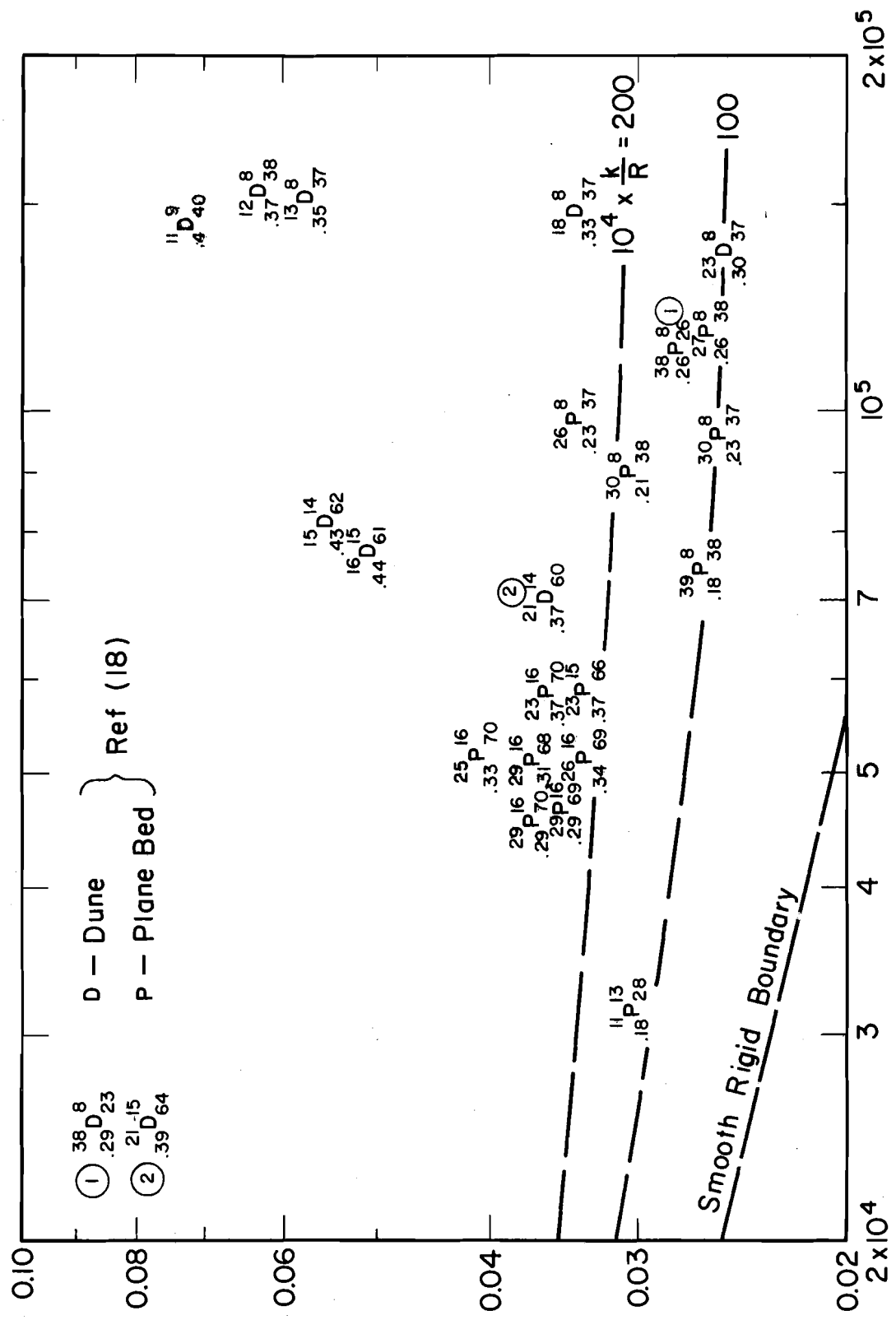
f
IR
D — Dune
P — Plane Bed
Ref (18)
$10^4 \times \frac{k}{R} = 200$
100
Smooth Rigid Boundary
$V_t / V_\tau > 10$
0.10
0.08
0.06
0.04
0.03
0.02
2×10^4
3
4
5
7
10^5
2×10^5

FIG. 4(c)

V. DISCUSSION OF RESULTS

Resistance Coefficient for Sand Bed Channels

As shown in Eq. 9, for steady flow in straight channels of constant width and slope with the bed covered by approximately uniform size sand, the Weisbach resistance coefficient f is a unique function of the Froude number, F, Reynolds number, R, particle size to hydraulic radius ratio, d_s/R, particle fall velocity to bed shear velocity ratio, V_t/V_τ, and the width-depth ratio. For a given discharge in such a channel, the resistance coefficient as well as the bed form is uniquely determined. In other words, the bed form is a function of the same parameters affecting f, i.e.,

$$\text{Bed form} = F_6 \left(F, R, \frac{d_s}{R}, \frac{V_t}{V_\tau}, \frac{B}{D}\right) \tag{16}$$

Equation 9 shows that the flow resistance is a six-dimensional problem and f can be determined without knowing the bed form. The fall velocity to shear velocity ratio, V_t/V_τ, accounts for the mobility of sediment particles in the flow and is essentially a convenient substitution for the instantaneous Reynolds number of the sediment to describe the effect due to viscosity of the fluid and the inertia of the sediment. The effects of the Froude number, Reynolds number, and bed shear—consequently that of V_t/V_τ— on bed form have been studied extensively (7, 33, 35). Nonetheless, the effects of the other two nondimensional parameters, d_s/R and B/D, has not been emphasized.

The width-depth ratio, B/D, represents the effect of geometry of the cross section. Its influence on the resistance coefficient or the bed form would not be underestimated if one realizes the emphasis on side-wall corrections made by many investigators (12, 20, 46). The presence of side walls creates a three-dimensional effect on the flow. As a result there are lateral velocity gradients and secondary currents; consequently, the bed patterns may be modified. This side-wall effect is particularly important when B/D is small.

Unfortunately, as discussed in the preceding chapter, the available data collected and analyzed in the present study consists of a small amount of experimental results with values of B/D less than 5. Consequently, no definite trend of the effect of B/D on f can be identified. However, preliminary analysis of the results do show obvious effects of the width-depth ratio, particularly for low values of B/D. Nevertheless, because of the insufficient amount of data in this report, the study of hydraulic resistance is limited to $B/D \geq 5$. Analyzed experimental results reveal that for $B/D > 5$, the effect due to change of values of B/D on f is relatively small and Eq. 9 can be simplified as

$$f = F_7 \left(\mathbb{F}, \mathbb{R}, \frac{d_s}{R}, \frac{V_t}{V_T}\right) \tag{17}$$

For subcritical flow with low $\mathbb{F}$ in sand bed channels, the wave resistance is relatively small in comparison to the form and surface resistances. Therefore, for a given value of Froude number f varies over a large range due to changes of values of $\mathbb{R}$, d_s/D, or V_t/V_T and the effect of $\mathbb{F}$ is relatively unimportant. In fact, if $\mathbb{F}$ is sufficiently

low, the physical phenomenon of the open-channel flow is quite similar to that for pipe flow with sand bed for which

$$f, \text{ Bed form} = F_{8,9}\left(R, \frac{d_s}{R}, \frac{V_t}{V_\tau}\right) \tag{18}$$

Contrarily, for supercritical flow and the high range of subcritical flow the wave resistance becomes relatively important. Consequently, the flow resistance is expected to depend heavily on the Froude number, particularly if the value of the Reynolds number is high.

Effect of Froude Number on Resistance Coefficient

As indicated in Eq. 17, the Weisbach resistance coefficient f varies with the Froude Number of the flow. Indeed, as shown in Fig. 1, for the range of the experiments analyzed, there is a definite relationship between f and F for a given value of d_s/R. For a constant d_s/R less than approximately 0.005, starting from a small value of F, the resistance coefficient-Froude number relationship shows that f increases rapidly with small increment of F, reaches a maximum and then decreases rapidly with increasing F until the Froude number approaches unity, then it increases again with F until another relatively small maximum is reached. For further increases in F the resistance coefficient decreases asymptotic to a constant value. This variation of f with F for a given d_s/R is obviously a result of the change of the bed configurations.

For small F with sufficiently slow flow so that there is no movement of bed materials, the plane bed configuration will remain if it was initially so. There is no form resistance due to irregularities of

bed form and the wave resistance is negligibly small. Consequently, the flow resistance is relatively small and the conventional Moody diagram is applicable if the corresponding value of surface roughness k can be determined.

As F increases movement of bed materials occurs and hence f increases. With the formation of ripples or dunes the flow becomes locally nonuniform and form resistance due to ripples or dunes develops. As a result the resistance coefficient increases rapidly with small increase in F. Yet as F is small and the sizes of the bed material and the ripples are small comparing to the depth of the flow, the wave resistance is still relatively small.

However, this rapid increase of f with F, which is due primarily to the form resistance caused by the ripples or dunes, cannot occur continuously without limit. With the formation of ripples or dunes the flow is locally accelerated at the upstream side of each ripple or dune and decelerated at its leeward side. As the height of the ripples or dunes increases, the pressure as well as the shear force increases near the crest of the ripples or dunes and the free surface profile will adjust accordingly, however small the adjustment is.

When the value of Froude number is small, increase in F implies more forces to move the sediment to form bigger and higher ripples or dunes until large pressure and shear near the crest preventing them from growing. Further increase in F implies a higher local flow velocity near the crest and hence a decrease in height of the ripples or dunes, and consequently decrease in f. Since the sediment particles are sufficiently small, eventually the plane bed configuration will occur again as the flow becomes faster and F approaches unity.

Further increase in F will result in formation of antidunes. The process on the size and height of antidunes as related to F is similar to that for ripples or dunes. Hence, it is clear that a second peak would occur on the f - F plot for a given d_s/R. However, because of the relatively rapid velocity of the flow with antidunes one can expect that the maximum value of f in the supercritical flow regime would be considerably smaller than that in the subcritical region.

If the sediment particles are very small, as shown by the double peak curve for $d_s/R = 10 \times 10^{-4}$ in Fig. 1, because of easiness of the sediment to be moved by the flow, and hence formation of ripples at low F, the resistance coefficient starts to increase rapidly at a relatively low F. Since the sediment is too easy to be removed from the crest of the ripples, the ripples cannot grow too high. Consequently, the two maximum values of f are relatively low, approximately 0.10 and 0.04 with $d_s/R = 10 \times 10^{-4}$ for the subcritical and supercritical regimes respectively, occurring at relatively low values of F, as shown in Fig. 1. Also, in the high F range of subcritical flow regime the plane bed configuration covers a relatively large range of F.

On the other hand, for larger particles, as shown by the curve with $d_s/R = 30 \times 10^{-4}$ in Fig. 1, because it requires more force to move a larger particle, f starts to increase rapidly with increasing F at a higher value of the Froude number for the larger sediment than for the smaller one. Since it is relatively difficult to push a heavy particle up the upstream slope of a dune, neither is it easy to entrain a heavy particle into the flow and then deposite it near the crest of the dune where the flow velocity is realtively high, one can expect that the dune

cannot grow too high either. Consequently, the maximum values of f can only be moderate, approximately 0.13 and 0.45 for $d_s/R = 30 \times 10^{-4}$, for the subcritical and supercritical regimes, respectively, occuring at higher respective values of F than for $d_s/R = 10 \times 10^{-4}$, as shown in Fig. 1. Also, because of the realtively lack of high mobility of the sediment in the flow, for high range of subcritical flow the plane bed covers a narrow range of approximately $F = 0.75 - 0.95$.

Thus, it is obvious that there is an optimum value of d_s/R for which at the appropriate F the bed form consists of dunes of proper height and length so that the value of f is a maximum among those for all d_s/R. From Fig. 1 it is seen that this optimum d_s/R is around 0.002 and the maximum f occurs at $F \approx 0.3$. It is interesting to observe from Fig. 1 that for small d_s/R, the 0.002 curve which gives the maximum f in the subcritical flow regime appears to give also the maximum f in the supercritical flow regime at $F \approx 1.1$.

If the sediment particles, and hence d_s/R, are sufficiently large, the ripple bed form will not develop. The bed form simply changes from plane bed to dunes as F increases. With reasons similar to those discussed previously for $d_s/R = 30 \times 10^{-4}$, the increase of f with F is relatively less rapid than for a smaller d_s/R, and the maximum value of f for a given d_s/R will be relatively small occuring at a higher F. Because of low mobility of the sediment there is no plane bed configuration for high Froude number range in the subcritical flow regime. In fact, as shown in Fig. 1 by the curve for $d_s/R = 70 \times 10^{-4}$, if d_s/R is sufficiently large, the peak of maximum f in the subcritical range of the f - F curve occurs at such a high F that there appears to be no second peak in the

supercritical flow regime. Physically, this fact implies that the bed form changes from dunes through an unstable and high energy loss transition region to antidunes without having the plane bed form occurring.

For large sediment particles, as shown by the curve for $d_s/R = 160 \times 10^{-4}$ in Fig. 1, although the basic value of f is high for both very high and very low values of the Froude number, for F between 0.5 and 1.5 not only the f - F curve has only one maximum f as for the case of $d_s/R = 70 \times 10^{-4}$ but also the maximum f is only approximately equal to 0.06, considerably smaller than that for $d_s/R = 70 \times 10^{-4}$. The relatively small maximum f is apparently due to the fact that large particles are relatively difficult to be moved against gravity and they receive relatively large drag force from the flow. Hence dunes or any bed form with large height generating large additional form and wave resistances cannot occur. Should the particles be so large that they are completely immovable by the flow, they would act as surface roughness elements on a rigid boundary and the corresponding f - F relationship simply shows the Froude number effect on f for that particular relative roughness (50).

In view of the dependence of f and bed form on F just discussed, and that f and bed form are both dependent variable on identical dependent parameters as shown in Eqs. 9 and 16, one would expect that regions corresponding to various bed forms can be identified in the f - F diagram. As shown in Fig. 1, experimental results confirm such expectation. For the high f region, with increasing F, the bed forms are successively ripples, dunes, transition, and antidunes. The low f region corresponds to plane bed configuration. Plane bed appears to occur over the entire range of Froude number in the subcritical flow regime, although

additional data within the range of F between 0.4 and 0.5 are desirable. To show further the continuity of the plane-bed region in f - F relationship, Fig. 2 is plotted to include data with B/D both greater and less than 5.

It should be mentioned here that, because of the limited amount of data available, the difference in measurement accuracy for different experiments, and the differences in definition in bed form terminologies, the dividing lines for the bed forms as well as the location of the curves for various values of d_s/R in Fig. 1 are more indicative than quantitative.

Experimental results as shown in Fig. 1 also confirm the relative importance of the Froude number on f as discussed in the preceding section. For flows with sufficiently high Froude number, the wave resistance becomes relatively dominant. Hence for a given F, the resistance coefficient is expected to vary within a small range. As shown in Fig. 1, in the supercritical flow regime, f approaches to a narrow range around 0.02 to 0.03 as F increases. For $F < 0.5$, f varies over a wide range for a given F. This is clearly due to the relatively low wave resistance and hence relatively negligible Froude number effect on f as discussed previously.

As shown in Eq. 17, there are actually two other parameters, R and V_t/V_τ, which affect the relationship between f and F. Nonetheless Fig. 1 shows that for the experiments analyzed the effects of these two parameters are relatively of secondary importance. Further discussion on this matter will be given in the following section.

Effect of Reynolds Number and V_t/V_τ on Resistance Coefficient

Although a unique relationship among f - $\mathbb{F}$ - d_s/R has been obtained from experimental results as shown in Fig. 1 and discussed in the preceding section, Eq. 17 indicates that the Reynolds number of the flow and the fall velocity to shear velocity ratio are two other parameters affecting the flow resistance. In fact, as discussed previously, for low Froude number, say less than 0.5, the wave resistance is relatively small. The effect of the presence of the free surface, and hence $\mathbb{F}$, on the resistance coefficient is negligible. Thus, approximately,

$$f = F_8 \left(\mathbb{R}, \frac{d_s}{R}, \frac{V_t}{V_\tau}\right) \tag{18}$$

In other words, a plot of f vs. $\mathbb{R}$ with d_s/R and V_t/V_τ as the other parmeters similar to the conventional Moody diagram will be sufficient to determine the resistant coefficient without considering the Froude number. Therefore, further clarification on the apparent puzzle that for low Froude number flow there is no influence of $\mathbb{F}$ on f in the f - $\mathbb{R}$ plot and yet $\mathbb{R}$ and V_t/V_τ impose negligible effect on the f - $\mathbb{F}$ diagram is warranted.

As discussed previously in the section on dimensional analysis, the parameter V_t/V_τ is actually a convenient combination of the nondimensional parameters ρ_s/ρ and S to indicate the relative mobility of the sediment near the channel bed. Since for the experiments analyzed the fluid is water and the sediment is sand, ρ_s/ρ is approximately constant. Therefore, V_t/V_τ actually indicates the effect of S which varied within a limited range between 0.000055 and 0.01079.

The Reynolds number represents the effect of viscosity of the fluid. If the value of the Reynolds number of the flow is sufficiently large, the flow is turbulent and the sand bed is definitely not smooth. Hence, the effect of change of R on f is expected to be small, if not negligible. For the data analyzed the Reynolds number ranged from 12,900 to 237,500 with very few points below 3×10^4. Thus by considering the ranges of R and V_t/V_τ for the data analyzed, it may reasonably be assumed that their combined effect on f is relative small as long as the parameter d_s/R accounts for the resistance due to boundary roughness and bed form. Therefore, a unique $f - F - d_s/R$ relationship is obtained as shown in Fig. 1.

In other words, if the Froude number of the flow is sufficiently low, the Reynolds number is sufficiently high, and V_t/V_τ varies within a limited range, the resistance to the flow is due primarily to the presence of the sediment producing both boundary roughness and bed form. Both the viscous surface resistance and wave resistance are comparatively negligible. Either the $f - F - d_s/R$ relationship as shown in Fig. 1 or Eq. 18 is approximately correct and sufficient to be used for describing f. The F in Fig. 1 and R and V_t/V_τ in Eq. 18 are simply the parameters describing the flow characteristics and the gravity effect on the two phases (fluid and sediment) and their effects on the bed form. Neither F nor R preserves its original physical meaning.

For low Froude number flows, in spite of the fact that Eq. 18 is a four-dimensional relationship, it has the advantage of direct correlation to flow containing sediment in pipes. In view of the large change in f for small change in F as shown in Fig. 1 one may expect a

study of f - ℝ relationship similar to the conventional Moody diagram would give better accuracy and reveal further details on hydraulic resistance in sand bed channels.

In particular, for the case of flow over plane bed, there is no problem in considering the mobility of the sediment in relationship to the formation of non-plane bed form and the corresponding form resistance. Therefore, the parameter V_t/V_τ would impose no appreciable effect on f and Eq. 18 can be simplified as

$$f = F_{10} \left(\mathbb{R}, \frac{d_s}{R}\right) \tag{19}$$

which is very similar to the Moody diagram relationship. In fact, since the channel bed is flat, as long as there is no appreciable surface wave resistance, the relationship as shown in Eq. 19 need not be restricted to low Froude number.

As shown in Fig. 3, analyzed data for plane-bed flows with $\mathbb{F}$ up to approximately unity appears to verify the unique relationship as indicated in Eq. 19. For a given d_s/R at low value of Reynolds number the f - ℝ relationship follows the curve on Moody diagram having the equivalent relative roughness. It should be noted here that numerically d_s/R does not equal k/R. As the value of ℝ increases the sediment starts to move and the flow resistance for plane-bed case is higher than that for the corresponding rigid boundary as additional energy is needed to transport the sediment. Consequently, the f - ℝ curve for the plane bed with a given d_s/R deviates from that for the rigid boundary and for a given ℝ the value of f is higher for the former. At the early stage of

deviation from the rigid boundary f - ℝ relationship, the value of f for the plane-bed flow decreases as ℝ increases. However, with more sediment in motion, for higher ℝ the value of f increases with the Reynolds number.

Corresponding to the trend for increasing k/R in the Moody diagram it is obvious that the family of the f - ℝ curves for the plane-bed case is such that for a given ℝ the larger d_s/R the larger the value of f as shown in Fig. 3. Physically this corresponds to (a) more energy is necessary to put the larger particles into motion, and (b) large d_s/R implies high boundary roughness.

Recently Lovera and Kennedy (33) obtained similar relationship for plane-bed hydraulic resistance. By including field data they covered a higher range of Reynolds number. However, they did not pay sufficient attention to the lower and upper limits of their f - ℝ curves. The pertinent portion of Lovera and Kennedy's result is plotted in Fig. 3 for comparison.

As mentioned previously for bed forms other than plane bed, in discussing the relationship between f and ℝ a restriction of low Froude number, say less than 0.5, is necessary so that relatively the effect due to wave resistance can be neglected and hence Eq. 18 applies approximately. For a given d_s/R in a flow with low 𝔽, although the f - ℝ relationship is approximately unique for the range of V_t/V_τ considered for plane bed as shown in Fig. 3, Eq. 18 shows that for flow with dunes and ripples f is also a function of V_t/V_τ.

Intuitively, for a large value of V_t/V_τ, the sediment particles are less mobile in the flow than for small V_t/V_τ; hence the bed will remain

longer to be plane with increasing R for the former than for the latter. Also, if dunes and ripples are found, for the same value of Reynolds number the height of the dunes or ripples, and consequently f, is smaller for larger V_t/V_τ than for small V_t/V_τ.

Conversely, for a given value of V_t/V_τ, which means the same degree of mobility of the sediment particles irrespect to their sizes, the larger the size, the more the form resistance. Consequently, for a given R and V_t/V_τ, f is higher for larger d_s/R than for the smaller one. A schematic plot of f as a function of R and d_s/R for low F is shown in Fig. 5. With a constant V_t/V_τ, as shown in Fig. 5, for a given d_s/R the f - R curve continues from that in the plane-bed region as shown in Fig. 3 into ripple or dune regions where f increases with increasing R for the range of R for flows in flumes or rivers.

For a constant V_t/V_τ, the bed form regions in the f - R plot can also be identified as shown schematically in Fig. 5 for the case of $V_t/V_\tau = b$. The location of the dividing lines for the bed-form regions will change if the value of V_t/V_τ changes. For instance, in Fig. 5 for $V_t/V_\tau = a$ the dividing lines will lie to the right side of the corresponding dividing lines for $V_t/V_\tau = b$ since $a > b$ implies the sediment is less mobile for case a than for b.

The anticipated relationship among f, R, d_s/R, and V_t/V_τ for flows with low values of Froude number as shown schematically in Fig. 5 is verified in a limited degree with flume experiments (Fig. 4). By comparison of the three plots for three different values of V_t/V_τ in Fig. 4 it can be seen that qualitative relationship as shown in Fig. 5

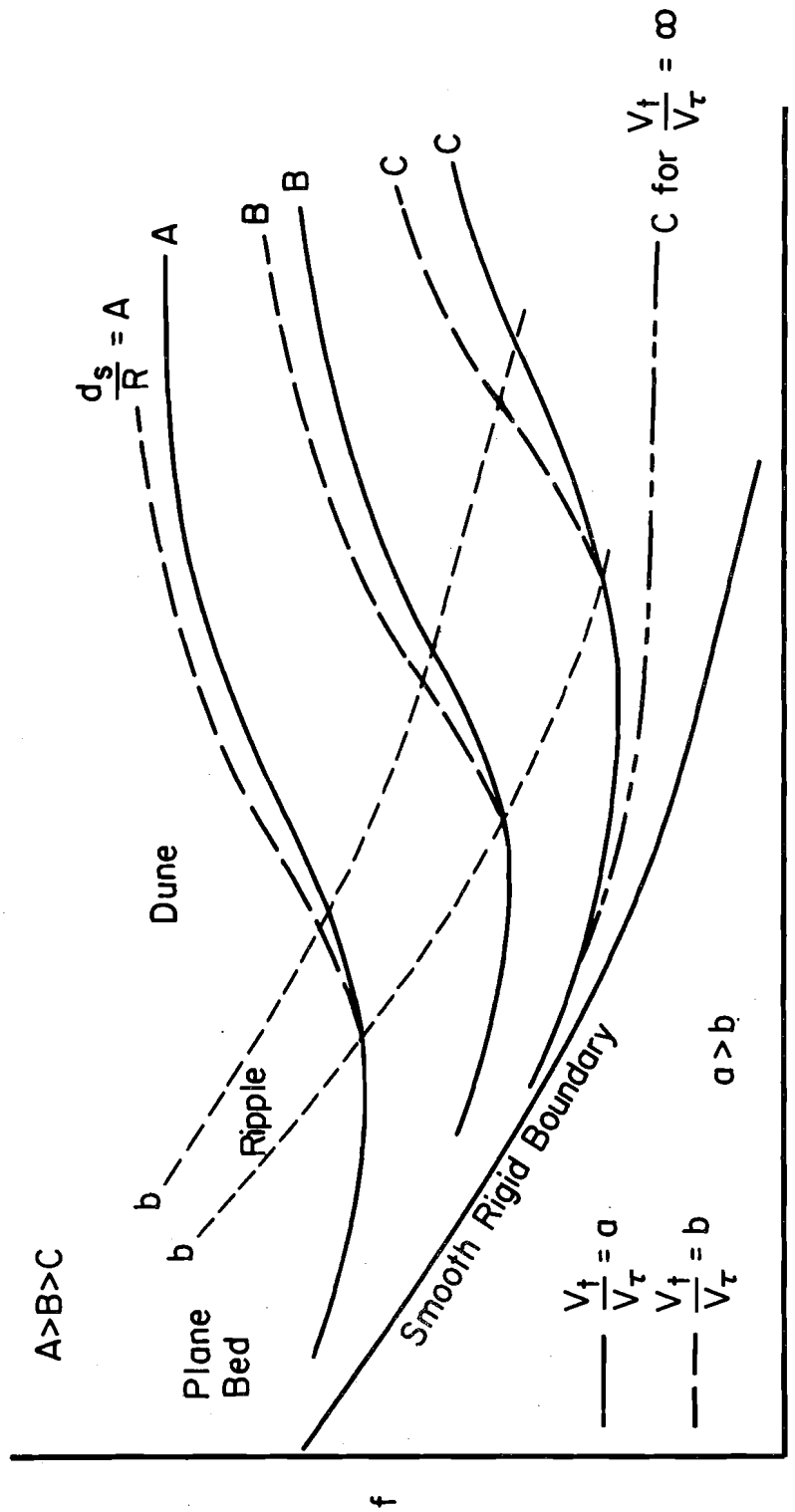

FIG. 5 RELATIONSHIP BETWEEN RESISTANCE COEFFICIENT AND REYNOLDS NUMBER AS FUNCTION OF d_s/R

agrees with the experimental results. However, more data is needed to give reliable quantitative description of Eq. 18.

Applications and Suggestions

The technique to determin the hydraulic resistance in sand-bed channel based on the results obtained in this study for engineering applications is rather simple. With sufficient data, a reliable diagram of the resistance coefficient f vs. Froude number of the flow, F for different values of d_s/R can be plotted. If the flow under consideration is approximately steady, uniform and two dimensional, the resistance coefficient f can be determined from Fig. 1 once the values of $F = V/\sqrt{gD}$ and d_s/R are computed. To determine f there is no need to know in advance the bed form of the channel which can also be found from Fig. 1. Further engineering computation and design can then be proceeded after f is known.

However, if the value of the Froude number of the flow is small, say for $F < 0.45$, better accuracy on the value of f can be obtained by using figures similar to Figs. 3 and 4. If from Fig. 1 it is indicated that the bed form is definitely flat, then Fig. 3 can be used to give the value of f with the value of the Reynolds number of the flow known. If the bed form is ripples or dunes, the value of V_t/V_τ has to be evaluated before Fig. 4 can be used to determine f.

The above technique for engineering applications, simple as it is, depends on the availability of sufficient amount of accurate data so that diagrams like Figs. 1, 3, and 4 can be plotted. Thus, it is obvious that more well-planned laboratory experiments are desirable. Moreover,

field data from natural rivers should also be analyzed to verify the validity of the technique proposed in this study and to cover a broader range of flow conditions.

Although natural rivers are usually wide in comparison to depth of flow, the cross-sectional shape effect on flow resistance nevertheless warrants further considerations. In particular, better knowledge in the effect of B/D may make possible development of improved methods for side-wall effect corrections and for correlation between field and laboratory data. Research on other geometric effects such as nonuniformity or curvalinear alignment of the channel as well as the effect of nonuniformity of the size of sediment particles is also highly desirable.

VI. CONCLUSIONS

Through dimensional analysis and analytical considerations based on concepts of fluid mechanics the hydraulic resistance to flow in sand-bed channels has been analyzed by using available experimental data and the following conclusions are drawn for flow of water having width to depth ratio greater than 5.

1. There is a unique and systematic relationship showing the Weisbach resistance coefficient f as a function of the Froude number of the flow and the sediment particle size to hydraulic radius ratio as shown in Fig. 1. The bed form which is also a dependent variable is also uniquely determined.

2. For flows with the Froude number around unity and higher, the wave resistance is a dominant factor in determining f while the effect due to changes of values of the Reynolds number of the flow, R, and particle fall velocity to shear velocity ratio, V_t/V_τ, is relatively negligible.

3. For flows with Froude number less than approximately 0.5, the wave resistance due to gravity and existance of the free surface is relatively small. Consequently, R and V_t/V_τ play a more important role in determining f for low Froude number flows than for high F. Unique relationships exist among f, R, d_s/R, and V_t/V_τ as shown in Figs. 4 and 5.

4. The plane bed form is continuous on the plot of f vs. $\mathbb{F}$, covering a wide range of $\mathbb{F}$ as shown in Figs. 1 and 2. For flows with plane bed the resistance coefficient f is only a function of $\mathbb{R}$ and d_s/R but not of V_t/V_T provided there is no appreciable wave resistance.

5. The technique and results obtained in this study appears to be simple for engineering applications. However, more reliable data, particularly those obtained from natural rivers are needed to determine accurate quantitative relationship between f and control parameters.

REFERENCES

1. Ackers, P., "Experiments on Small Streams in Alluvium," Jour. Hydraulics Div., ASCE, Vol. 90, No. HY4, pp. 1-37, July, 1964; Closure, Jour. Hydraulics Div., ASCE, Vol. 92, No. HY2, pp. 329-345, March, 1966.

2. Bagnold, R. A., "Some Flume Experiments on Large Grains but Little Denser than the Transporting Fluid, and their Implications," Proc., Inst. of Civil Engrs., Vol. 4, Pt. 3, pp. 174-205, April, 1955.

3. Bagnold, R. A., "An Approach to the Sediment Transport Problem from General Physics," U.S. Geol. Survey, Prof. Paper 422-I, 1966.

4. Barton, J. R. and Lin, P. N., "A Study of Sediment Transport in Alluvial Channels," Rept. No. 55JRB2, Civil Eng. Dept., Colorado State Univ., Fort Collins, March, 1955.

5. Blench, T., Mobile-Bed Fluviology, 2nd Ed., Univ. Alberta Press, 1969.

6. Blench, T., and Qureshi, M. A. "Practical Regime Analysis of River Slopes," Jour. Hydraulics Div., ASCE, Vol. 90, No. HY2, pp. 81-98, March, 1964.

7. Bogardi, J. L., "European Concepts of Sediment Transportation," Jour. Hydraulics Div., ASCE, Vol. 91, No. HY1, pp. 29-54, Jan., 1965.

8. Brooks, N. H., "Mechanics of Streams with Movable Beds of Fine Sand," Trans. ASCE, Vol. 123, pp. 526-594, 1958.

9. Chien, N., "The Present Status of Research on Sediment Transport," Trans. ASCE, Vol. 121, pp. 833-868, 1956.

10. Colby, B. R., "Discharge of Sands and Mean-Velocity Relationships in Sand-Bed Streams," U.S. Geol. Survey, Prof. Paper 462-A, 1964.

11. Einstein, H. A., "Formulas for the Transportation of Bed Load," Trans. ASCE, Vol. 107, pp. 561-577, 1942.

12. Einstein, H. A., "The Bed Load Function for Sediment Transportation in Open-Channel Flows," Tech. Bull. No. 1026, Soil Conservation Service, U.S. Dept. of Agri., 1950.

13. Einstein, H. A. and Barbarossa, N. L., "River Channel Roughness," Trans. ASCE, Vol. 117, pp. 1121-1146, 1952.

14. Engelund, F., "Hydraulic Resistance of Alluvial Streams," Jour. Hydraulics Div., ASCE, Vol. 92, HY2, pp. 315-326, March, 1966.

15. Garde, R. J., and Ranga Raju, K. G., "Regime Criteria for Alluvial Streams," Jour. Hydraulics Div., ASCE, Vol. 89, No. HY6, pp. 153-164, Nov., 1963.

16. Grade, R. J., and Ranga Raju, K. G., "Resistance Relationship for Alluvial Channel Flow," Jour. Hydraulics Div., ASCE, Vol. 92, No. HY4, pp. 77-100, July, 1966.

17. Gilbert, G. K., "Transportation of Debris by Running Water," U.S. Geol. Survey, Prof. Paper 86, 1914.

18. Guy, H. P., Simons, D. B., and Richardson, E. V., "Summary of Alluvial Channel Data from Flume Experiments, 1956-61," U.S. Geol. Survey, Prof. Paper 462-I, 1966.

19. Haynie, R. M., and Simons, D. B., "Design of Stable Channels in Alluvial Materials," Jour. Hydraulics Div., ASCE, Vol. 94, No. HY6, pp. 1399-1420, Nov., 1968.

20. Johnson, J. W., "The Importance of Considering Side-Wall Friction in Bed Load Investigations," Civil Engineering, Vol. 12, No. 6, pp. 329-331, June, 1942.

21. Johnson, J. W., "Laboratory Investigations on Bed-Load Transportation and Bed Roughness," Rept., SCS-TP-50, Soil Conservation Service, U.S. Dept. of Agri., March 1943.

22. Kalinske, A. A., "The Movement of Sediment as Bed Load in Rivers," Trans., AGU, Vol. 28, pp. 615-620, 1947.

23. Kennedy, J. F., "Stationary Waves and Antidunes in Alluvial Channels," Rept. No. KH-R-2, W. M. Keck Lab. of Hydraulics and Water Resources, Calif. Inst. of Tech., Jan., 1961.

24. Kennedy, J. F., "Further Laboratory Studies of the Roughness and Suspended Load of Alluvial Streams," Rept. No. KH-R-3, W. M. Keck Lab. of Hydraulics and Water Resources, Calif. Inst. Tech., Jan., 1961.

25. Kennedy, J. F., "The Mechanics of Dunes and Antidunes in Erodible-Bed Channels," J. of Fluid Mech., Vol. 16, Pt. 4, pp. 521-544, 1963.

26. Lacey, G., "A General Theory of flow in Alluvium," Proc., Inst. of Civil Engrs., London, Vol. 27, No. 1, 1946.

27. Langbein, W. B., "Hydraulic Criteria for Sand-Waves," Trans., AGU, Vol. 23, Pt. 2, pp. 615-618, 1942.

28. Langbein, W. B., "Geometry of River Channels," Jour. Hydraulics Div., ASCE, Vol. 90, No. HY2, pp. 301-312, March, 1964.

29. Laursen, E. M., "The Total Sediment Load of Streams," Jour. Hydraulics Div., ASCE, Vol. 84, No. HY1, pp. 1530(1-36), Jan., 1958.

30. Leopold, L. B., and Maddock, T., Jr., "The Hydraulic Geometry of Stream Channels and Some Physiographic Implications," U.S. Geol. Survey, Prof. Paper 252, 1953.

31. Liu, H. K., "Mechanics of Sediment-Ripple Formation," Jour. Hydraulics Div., ASCE, Vol. 83, No. HY2, pp. 1197(1-23), April, 1957.

32. Liu, H. K., Hwang, S. Y., "Discharge Formula for Straight Alluvial Channels," Trans., ASCE, Vol. 126, pp. 1787-1822, 1961.

33. Lovera, F. and Kennedy, J. F., "Friction-Factors for Flat-Bed Flows in Sand Channels," Jour. Hydraulics Div., ASCE, Vol. 95, No. HY4, pp. 1227-1234, July, 1969.

34. Meyer-Peter, E., and Muller, R., "Formulas for Bed-Load Transport," Int'l. Assoc. of Hydr. Structures Res., Proc. 2nd Meeting, Stokholm, pp. 39-64, 1948.

35. Raudkivi, A. J., Loose Boundary Hydraulics, pp. 222-252, Pergamon Press, New York, 1967.

36. Raudkivi, A. J., "Analysis of Resistance in Fluvial Channels," Jour. Hydraulic Div., ASCE, Vol. 93, No. HY5, pp. 73-84, Sept., 1967.

37. Rouse, H., "Critical Analysis of Open-Channel Resistance," Jour. Hydraulics Div., ASCE, Vol. 91, No. HY4, pp. 1-25, July, 1965.

38. Shen, H. W., "Development of Bed Roughness in Alluvial Channels," Jour. Hydraulic Div., ASCE, Vol. 88, No. HY3, pp. 45-58, May, 1962.

39. Simons, D. B., "Theory and Design of Stable Channels in Alluvial Materials," Rept. No. CER57 DBS17, Colorado State Univ., 1957.

40. Simons, D. B., and Richardson, E. V., "Resistance to Flow in Alluvial Channels," Trans., ASCE, Vol. 127, Pt. 1, pp. 927-1006, 1962.

41. Simons, D. B., and Richardson, E. V., "Forms of Bed Roughness in Alluvial Channels," Trans., ASCE, Vol. 128, Pt. 1, pp. 284-302, 1963.

42. Simons, D. B., and Richardson, E. V. "Resistance to Flow in Alluvial Channels," U.S. Geol. Survey, Prof. Paper 422-J, 1966.

43. Smith, K.V.H., "Alluvial Channel Resistance Related to Bed Form," Jour. Hydraulics Div., ASCE, Vol. 94, No. HY1, pp. 59-69, Jan., 1968.

44. Stein, R. A., "Laboratory Studies of Total Load and Apparent Bed Load," Jour. Geophy. Res., Vol. 70, No. 8, pp. 1831-1842, April, 1965.

45. Vanoni, V. A., "Transportation of Suspended Sediment by Water," Trans., ASCE, Vol. 111, pp. 67-102, 1946.

46. Vanoni, V. A., and Brooks, N. H., "Laboratory Studies of the Roughness and Suspended Load of Alluvial Streams," Rept. No. E-68, Sedimentation Lab., Calif. Inst. of Tech., Dec. 1957.

47. Vanoni, V. A., and Hwang, L.-S., "Relation between Bed Forms and Friction in Streams," Jour. Hydraulics Div., ASCE, Vol. 93, No. HY3, pp. 121-144, May, 1967.

48. Vanoni, V. A., and Nomicos, G. N., "Resistance Properties of Sediment-Laden Streams," Trans., ASCE, Vol. 125, Pt. 1, pp. 284-323, 1960.

49. Yalin, M. S., "An Expression for Bed-Load Transportation," Jour. Hydraulics Div., ASCE, Vol. 89, No. HY1, pp. 221-250, May, 1963.

50. Yen, B. C., Discussion of "Large-Scale Roughness in Open-Channel Flow," Jour. Hydraulics Div., ASCE, Vol. 91, No. HY5, pp. 257-262, Sept., 1965.

51. Yen, B. C., and Wenzel, H. G., "Dynamic Equations for Steady Spatially Varied Flow," Submitted to Jour. Hydraulics Div., ASCE, for publication.

APPENDIX

TABLE OF DATA EVALUATED

(1) Colorado State University, Ref. (18) 8-ft flume

A. d_s = 0.19 mm V_t = 0.103 fps

Run No.	Q cfs	D ft	R ft	S $\times 10^5$	V fps	V_T fps	f	R	F	B/D	V_t/V_T	d_s/R $\times 10^4$	Bed Form
24	6.52	0.94	0.76	5.5	0.87	0.037	0.0143	59000	0.16	8.5	2.80	8.2	Plane
22A	2.99	0.48	0.43	10	0.78	0.037	0.0177	28700	0.20	16.7	2.80	14.5	Plane
2	6.68	1.06	0.84	15	0.79	0.064	0.0525	49500	0.14	7.5	1.61	7.4	Ripple
22B	2.99	0.43	0.39	16	0.87	0.042	0.0186	29300	0.23	18.6	2.44	16.0	Plane
26	2.00	0.30	0.28	17	0.83	0.040	0.0186	20900	0.27	26.7	2.60	22.3	Plane
25	6.45	0.93	0.75	18	0.87	0.066	0.0460	58500	0.16	8.6	1.58	8.3	Ripple
22C	2.99	0.42	0.38	18	0.89	0.047	0.0223	29400	0.24	19	2.21	16.4	Plane
30	8.91	1.00	0.80	28	1.11	0.085	0.0468	75900	0.20	8	1.22	7.8	Ripple
1	3.42	0.58	0.51	34	0.74	0.075	0.0822	28800	0.17	13.8	1.37	12.2	Ripple
31	10.62	1.02	0.81	43	1.30	0.106	0.0532	92500	0.23	7.85	0.97	7.7	Ripple
27	4.08	0.55	0.48	57	0.93	0.093	0.080	43600	0.22	14.5	1.10	13.0	Ripple
5	12.67	1.03	0.82	58	1.54	0.124	0.0518	106000	0.27	7.77	0.84	7.6	Ripple
23	2.99	0.44	0.40	62	0.85	0.089	0.0877	29600	0.23	18.2	1.16	15.6	Ripple
32	13.64	0.95	0.77	66	1.79	0.128	0.0410	121500	0.32	8.43	0.81	8.6	Dune
8	14.81	0.93	0.75	70	1.99	0.135	0.0368	132000	0.36	8.6	0.76	8.3	Dune
28	4.49	0.54	0.48	79	1.04	0.110	0.0910	43700	0.25	14.8	0.93	13.0	Ripple
33	16.66	1.06	0.84	83	1.96	0.150	0.0467	142000	0.34	7.55	0.69	7.4	Dune
29	5.08	0.56	0.49	84	1.13	0.115	0.0830	49800	0.27	14.3	0.89	14.4	Ripple

(1) A. cont'd.

Run No.	Q cfs	D ft	R ft	S $\times 10^5$	V fps	V_T fps	f	R	F	B/D	V_t/V_T	d_s/R $\times 10^4$	Bed Form
3	5.20	0.55	0.49	92	1.18	0.121	0.0843	43000	0.28	14.5	0.85	14.4	Ripple
11	20.47	1.09	0.86	99	2.35	0.165	0.0393	182000	0.40	7.34	0.63	7.3	Dune
13	21.98	0.89	0.73	100	3.09	0.153	0.0196	122500	0.58	9	0.68	8.5	Transition
14	22.12	0.86	0.71	106	3.22	0.155	0.0185	207000	0.61	9.3	0.67	8.8	Transition
15	21.84	0.79	0.66	112	3.46	0.154	0.0158	207500	0.69	10.1	0.67	9.4	Plane
34	7.00	0.52	0.46	127	1.68	0.133	0.0500	65000	0.41	15.4	0.75	13.5	Dune
12	21.96	1.02	0.81	130	2.69	0.185	0.0378	200000	0.47	7.85	0.57	7.7	Dune
6	8.14	0.61	0.53	130	1.67	0.149	0.0644	71800	0.38	13.1	0.69	11.8	Dune
7	9.66	0.68	0.58	140	1.78	0.162	0.0633	90600	0.38	11.8	0.64	10.7	Dune
35	7.52	0.52	0.46	147	1.81	0.148	0.0535	74000	0.44	15.4	0.70	13.5	Dune
16	22.14	0.72	0.61	156	3.84	0.175	0.0166	210000	0.80	11.1	0.59	10.2	Transition
10	11.68	0.51	0.45	170	2.89	0.157	0.0237	117000	0.71	15.7	0.66	13.9	Plane
9	8.22	0.49	0.44	194	2.10	0.166	0.0500	81500	0.53	16.3	0.63	14.2	Dune
17	22.19	0.67	0.58	196	4.14	0.192	0.0171	217000	0.89	11.9	0.54	10.7	Antidune
18	22.16	0.64	0.55	300	4.33	0.233	0.0231	217500	0.95	12.5	0.45	11.3	Antidune
19	22.19	0.64	0.55	350	4.33	0.249	0.0264	213000	0.95	12.5	0.41	11.3	Antidune
39	22.33	0.61	0.53	390	4.58	0.258	0.0253	217500	1.03	13.1	0.40	11.8	Antidune
20	1.04	0.60	0.52	460	4.62	0.278	0.029	213000	1.05	13.3	0.37	12.0	Antidune
21	1.25	0.50	0.44	542	4.03	0.277	0.0377	158000	1.00	16	0.38	14.2	Antidune
38	1.07	0.58	0.51	582	4.74	0.309	0.0339	211000	1.10	13.8	0.33	12.2	Antidune
36	1.22	0.51	0.45	845	3.81	0.350	0.0675	145500	0.94	15.7	0.30	13.8	Chute-pool
37	0.96	0.65	0.56	950	4.20	0.414	0.0778	203000	0.92	12.3	0.25	11.1	Chute-pool

(1) cont'd.

B. d_s = 0.27 mm V_t = 0.192 fps

Run No	Q cfs	D ft	R ft	S $\times 10^5$	V fps	V_τ fps	f	R	F	B/D	V_t/V_τ	d_s/R $\times 10^4$	Bed Form
50A	6.09	0.96	0.775	7	0.79	0.042	0.0227	49000	0.14	8.32	4.53	11.4	Plane
50D	6.09	0.91	0.741	18	0.84	0.066	0.0493	51300	0.16	8.79	2.90	12.0	Ripple
51	9.86	0.99	0.793	46	1.24	0.108	0.0607	82000	0.22	8.08	1.77	11.2	Ripple
52	12.25	0.94	0.760	65	1.63	0.126	0.0477	103000	0.30	8.52	1.52	11.7	Ripple
54	13.62	0.93	0.755	84	1.83	0.143	0.0488	122000	0.33	8.60	1.33	11.7	Dune
53	15.58	1.02	0.813	108	1.91	0.168	0.0618	153000	0.33	7.84	1.14	10.9	Dune
57	5.11	0.48	0.430	126	1.33	0.133	0.0800	45000	0.34	16.3	1.45	22.5	Ripple
56	11.09	0.75	0.630	126	1.85	0.159	0.0591	95500	0.38	10.7	1.20	14.1	Dune
55	17.80	1.08	0.850	130	2.06	0.189	0.0673	153500	0.35	7.41	1.01	10.4	Dune
45	21.84	0.84	0.690	138	3.25	0.175	0.0232	195000	0.62	9.53	1.09	12.8	Transition
43	19.23	1.13	0.88	140	2.13	0.200	0.0705	162000	0.35	7.08	0.96	10.1	Dune
44	21.55	1.03	0.82	163	2.62	0.208	0.0504	182000	0.45	7.76	0.92	10.8	Dune
42	15.68	0.94	0.76	167	2.09	0.202	0.0745	128000	0.38	8.52	0.95	11.7	Dune
46	21.76	0.74	0.625	167	3.68	0.183	0.0198	205000	0.75	10.8	1.05	14.2	Plane
58	6.75	0.46	0.412	185	1.83	0.157	0.0590	59700	0.48	17.4	1.22	21.5	Dune
47	21.79	0.63	0.545	280	4.32	0.221	0.0209	184000	0.96	12.7	0.86	16.3	Antidune
48	21.69	0.59	0.513	493	4.60	0.285	0.0307	196000	1.06	13.6	0.67	17.3	Antidune
39	21.71	0.55	0.482	813	4.93	0.355	0.0415	169000	1.17	14.6	0.54	18.4	Antidune
41	15.41	0.45	0.404	952	4.28	0.352	0.054	125000	1.12	17.8	0.54	21.9	Chute-pool
40	21.35	0.60	0.523	1,022	4.45	0.415	0.0695	169000	1.01	13.3	0.46	16.9	Chute-pool

(1) cont'd.

C. d_s = 0.28 mm V_t = 0.205 fps

Run No.	Q cfs	D ft	R ft	S x10^5	V fps	V_T fps	f	R	F	B/D	V_t/V_T	d_s/R x10^4	Bed Form
7	6.61	1.01	0.807	7	0.82	0.043	0.0220	52000	0.14	7.92	4.78	11.4	Plane
8	7.76	1.00	0.800	11	0.97	0.054	0.0248	58000	0.17	8.0	3.84	11.5	Plane
9	7.76	1.01	0.807	23	0.96	0.077	0.0515	56000	0.17	7.92	2.61	11.4	Ripple
10	4.16	0.59	0.513	41	0.88	0.082	0.0695	36700	0.20	13.6	2.50	17.9	Ripple
5	10.73	1.00	0.80	45	1.34	0.107	0.0510	90000	0.24	8.0	1.91	11.5	Ripple
13	13.46	1.00	0.80	63	1.68	0.127	0.0457	113500	0.30	8.0	1.62	11.5	Ripple
4	10.73	0.86	0.701	69	1.56	0.125	0.0513	88000	0.30	9.3	1.69	13.0	Ripple
11	4.92	0.59	0.513	73	1.04	0.110	0.0896	43500	0.24	13.6	1.86	17.9	Ripple
33	15.74	1.06	0.837	90	1.86	0.155	0.0555	135500	0.32	7.55	1.31	11.0	Dune
1	12.70	0.88	0.72	100	1.80	0.152	0.0570	110000	0.34	9.1	1.34	12.8	Dune
12	7.19	0.57	0.50	108	1.58	0.132	0.0558	65800	0.37	14.0	1.56	18.4	Ripple
14	8.61	0.62	0.537	116	1.74	0.141	0.0525	77300	0.39	12.9	1.45	17.1	Dune
20	18.14	1.05	0.832	120	2.16	0.179	0.0550	148500	0.37	7.62	1.14	11.0	Dune
2	15.19	0.92	0.748	131	2.06	0.178	0.0597	127000	0.38	8.7	1.15	12.3	Dune
21	20.39	1.07	0.844	131	2.38	0.188	0.050	169000	0.41	7.47	1.09	10.9	Dune
19	9.90	0.65	0.56	134	1.90	0.155	0.0533	86500	0.42	12.3	1.32	16.4	Dune
16	17.23	1.02	0.812	134	2.11	0.187	0.063	141300	0.37	7.84	1.10	11.3	Dune
23	22.02	0.91	0.74	134	3.02	0.179	0.0281	184500	0.56	8.8	1.15	12.4	Transition
17	10.01	0.65	0.56	136	1.92	0.157	0.0535	86700	0.42	12.3	1.31	16.4	Dune
3	15.28	0.88	0.72	136	2.17	0.177	0.0535	128000	0.41	9.1	1.16	12.8	Dune

(1) C. cont'd.

Run No.	Q cfs	D ft	R ft	S $\times 10^5$	V fps	V_τ fps	f	R	F	B/D	V_t/V_τ	d_s/R $\times 10^4$	Bed Form
18	11.96	0.61	0.53	141	2.45	0.155	0.032	104700	0.55	13.1	1.33	17.3	Dune
30	15.68	0.64	0.551	142	3.06	0.159	0.0216	135000	0.67	12.5	1.29	16.7	Transition
34	5.50	0.44	0.396	150	1.56	0.139	0.0635	49000	0.41	18.2	1.49	23.2	Dune
22	14.92	0.60	0.523	153	3.11	0.161	0.0214	124500	0.71	13.3	1.28	17.6	Plane
15	12.87	0.75	0.630	158	2.14	0.179	0.056	103600	0.44	10.7	1.15	14.6	Dune
24	21.98	0.82	0.680	172	3.35	0.194	0.0268	188000	0.65	9.76	1.05	13.5	Transition
25	21.85	0.72	0.610	199	3.79	0.198	0.0218	186500	0.79	11.1	1.03	15.1	Plane
28	15.72	0.55	0.485	229	3.57	0.189	0.0224	140500	0.85	14.5	1.09	18.9	Plane
29	15.70	0.52	0.46	278	3.77	0.203	0.0232	133000	0.92	15.4	1.01	20.0	Plane
26	15.51	0.50	0.445	328	3.88	0.217	0.025	140000	0.97	16.0	0.94	20.6	Antidune
32	21.76	0.58	0.428	470	4.69	0.254	0.0234	145300	1.09	16.7	0.80	21.5	Antidune
27	15.47	0.43	0.388	533	4.50	0.258	0.0263	142000	1.21	18.6	0.80	23.7	Antidune
31	21.34	0.56	0.490	593	4.76	0.306	0.033	156500	1.12	14.3	0.67	18.7	Antidune
35	21.33	0.54	0.476	815	4.93	0.353	0.0410	170000	1.18	14.8	0.59	19.3	Antidune
37	8.34	0.30	0.279	820	3.48	0.271	0.0485	72000	1.12	26.7	0.76	32.9	Antidune
38	15.26	0.40	0.364	930	4.77	0.320	0.036	127000	1.33	20.0	0.62	25.2	Chutepool
36	21.38	0.57	0.50	1007	4.69	0.403	0.059	172500	1.09	14.0	0.51	18.4	Chutepool

(1) cont'd.

D. d_s = 0.45 mm V_t = 0.532 fps

Run No.	Q cfs	D ft	R ft	S $\times 10^5$	V fps	V_τ fps	f	R	F	B/D	V_t/V_τ	d_s/R $\times 10^4$	Bed Form
14	3.94	0.61	0.53	15	0.81	0.050	0.0305	30700	0.18	13.1	10.6	27.9	Plane
13	1.84	0.35	0.321	19	0.65	0.044	0.0367	14300	0.19	22.9	12.1	46.1	Plane
17	6.22	0.98	0.784	20	0.80	0.064	0.0513	46700	0.14	8.2	8.4	18.9	Ripples
16	5.11	0.81	0.672	21	0.79	0.061	0.0477	39700	0.15	9.9	8.7	22.0	Ripples
15	5.07	0.80	0.667	23	0.79	0.070	0.0628	38200	0.16	10.0	7.58	22.2	Ripples
18	3.62	0.58	0.56	31	0.78	0.075	0.074	32200	0.18	13.8	7.12	26.4	Ripples
2	7.90	0.82	0.678	36	1.20	0.088	0.0595	59000	0.23	9.8	6.03	21.8	Ripples
3	7.90	0.85	0.702	39	1.16	0.094	0.0525	60000	0.22	9.4	5.85	21.1	Ripples
9	3.84	0.55	0.485	40	0.88	0.079	0.0645	31900	0.21	14.5	6.75	30.5	Ripples
1	7.85	0.80	0.667	42	1.23	0.095	0.0477	56300	0.24	10	5.83	22.2	Ripples
5	7.93	0.75	0.63	47	1.32	0.098	0.0841	60200	0.27	10.7	5.42	23.5	Ripples
11	1.95	0.35	0.321	49	0.70	0.071	0.0823	16500	0.21	22.9	7.50	46.1	Ripples
4	7.94	0.69	0.588	57	1.44	0.104	0.0417	60000	0.31	11.6	5.10	25.2	Dune
8	3.83	0.51	0.452	60	0.93	0.093	0.0800	31300	0.23	15.7	5.71	32.7	Ripples
7	7.98	0.70	0.597	78	1.43	0.123	0.0592	62800	0.30	11.4	4.33	24.8	Dune
10	1.95	0.33	0.305	88	0.75	0.093	0.123	16500	0.23	24.2	5.71	48.5	Ripples
6	3.90	0.46	0.412	88	1.07	0.108	0.0815	30800	0.28	17.4	4.93	35.9	Ripples
12	1.95	0.29	0.27	106	0.85	0.096	0.1020	17000	0.28	27.6	5.57	54.8	Ripples

(1) D. cont'd.

Run No.	Q cfs	D ft	R ft	S $\times 10^5$	V fps	V_τ fps	f	R	F	B/D	V_t/V_τ	d_s/R $\times 10^4$	Bed Form
19	4.24	0.41	0.372	112	1.30	0.116	0.0637	42400	0.36	19.5	4.58	39.8	Dune
21	12.12	0.96	0.777	114	1.58	0.169	0.0915	102300	0.28	8.3	3.15	19.1	Dune
22	13.54	1.00	0.80	124	1.70	0.179	0.0885	112400	0.30	8.0	2.97	18.5	Dune
25	4.91	0.42	0.381	189	1.47	0.152	0.0855	47800	0.40	19.0	3.50	38.9	Dune
20	8.14	0.61	0.53	193	1.68	0.182	0.0938	75000	0.38	13.1	2.92	27.9	Dune
23	13.34	0.65	0.56	247	2.57	0.211	0.0540	120000	0.56	12.3	2.53	35.9	Dune
24	8.73	0.62	0.537	289	1.76	0.223	0.1282	80700	0.39	12.9	2.38	27.6	Dune
40	21.41	0.81	0.672	301	3.32	0.255	0.0472	201000	0.65	9.9	2.09	22.0	Dune
39	20.64	0.55	0.485	364	4.71	0.239	0.0206	206000	1.12	14.5	2.23	30.5	Standing Wave
26	14.45	0.34	0.314	366	5.38	0.192	0.0102	144500	1.63	23.5	2.77	47.1	Plane
28	11.19	0.40	0.364	366	3.52	0.207	0.0277	107000	0.98	20	2.57	40.7	Transition
29	4.54	0.30	0.279	369	1.89	0.182	0.0742	45500	0.61	26.7	2.92	53.1	Dune
31	14.85	0.44	0.396	432	4.24	0.234	0.0244	144500	1.13	18.2	2.27	37.4	Standing Wave
27	7.91	0.33	0.305	436	2.99	0.207	0.0383	80000	0.92	24.2	2.57	48.5	Transition
36	3.15	0.19	0.182	446	2.04	0.162	0.0505	33400	0.82	42.1	3.30	81.3	Transition
41	21.62	0.54	0.476	466	5.05	0.268	0.0226	214000	1.21	14.8	1.99	31.1	Standing Wave
30	5.33	0.27	0.253	492	2.47	0.200	0.0525	54000	0.84	29.6	2.66	58.5	Transition
35	5.58	0.25	0.235	494	2.80	0.193	0.038	56200	0.99	32	2.76	63.0	Transition
34	8.44	0.28	0.267	546	3.73	0.217	0.0271	85700	1.24	28.6	2.46	55.4	Standing Wave

(1) D. cont'd.

Run No.	Q cfs	D ft	R ft	S $\times 10^5$	V fps	V_τ fps	f	R	F	B/D	V_t/V_τ	d_s/R $\times 10^4$	Bed Form
33	10.02	0.27	0.253	607	4.60	0.223	0.0188	97000	1.56	29.6	2.39	58.5	Standing Wave
38	21.38	0.50	0.444	619	5.38	0.298	0.0246	215000	1.34	16	1.79	33.3	Standing Wave
37	18.87	0.43	0.388	620	5.54	0.279	0.0203	192000	1.49	18.6	1.91	38.2	Transition
32	14.96	0.37	0.339	656	5.03	0.268	0.0227	150000	1.46	21.6	2.02	43.7	Antidune
45	5.58	0.28	0.261	862	2.50	0.269	0.0927	58900	0.83	28.6	1.98	56.7	Antidune
44	10.83	0.28	0.261	898	4.78	0.275	0.0265	113000	1.59	28.6	1.90	56.7	Antidune
42	13.43	0.31	0.288	986	5.36	0.303	0.0256	142800	1.70	25.8	1.76	51.4	Antidune
43	21.42	0.43	0.388	1010	6.18	0.356	0.0266	215000	1.66	18.6	1.49	38.2	Antidune

E. d_s = 0.47 mm V_t = 0.579 fps

Run No.	Q cfs	D ft	R ft	S $\times 10^5$	V fps	V_τ fps	f	R	F	B/D	V_t/V	d_s/R $\times 10^4$	Bed Form
46	14.54	1.11	0.869	84	1.64	0.153	0.0696	109500	0.27	7.2	3.79	17.7	Dunes
47	9.59	0.75	0.63	42	1.60	0.093	0.0270	74100	0.33	10.7	6.22	24.5	Dunes
48	15.26	1.23	0.941	52	1.55	0.126	0.0528	107600	0.25	6.5	4.60	16.4	Dunes
49	21.32	1.33	1.00	173	2.00	0.236	0.111	145000	0.31	6.0	2.45	15.4	Dunes
85	7.11	0.78	0.65	47	1.13	0.100	0.0626	56000	0.23	10.3	5.79	23.7	Ripples
86	6.92	0.76	0.64	46	1.14	0.098	0.0592	62500	0.23	10.5	5.91	24.1	Ripples
87	6.96	0.75	0.63	46	1.16	0.096	0.0548	66000	0.24	10.7	6.03	24.5	Ripples
88	7.10	0.74	0.625	49	1.20	0.099	0.0545	66300	0.25	10.8	5.85	24.7	Ripples
90	6.97	0.60	0.523	53	1.45	0.094	0.0336	65000	0.33	13.3	6.16	29.5	Ripples

(1) E. cont'd.

Run No.	Q cfs	D ft	R ft	S $\times 10^5$	V fps	V_τ fps	f	R	F	B/D	V_t/V_τ	d_s/R $\times 10^4$	Bed Form
89	7.08	0.60	0.523	65	1.47	0.106	0.0416	68700	0.33	13.3	5.46	29.5	Ripples
93	7.20	0.62	0.537	72	1.45	0.112	0.0477	62700	0.32	12.9	5.17	28.7	Dunes
92	7.14	0.63	0.544	90	1.43	0.126	0.0620	69600	0.32	12.7	4.60	28.3	Dunes
91	7.12	0.58	0.508	117	1.53	0.139	0.0660	68100	0.35	13.8	4.17	30.3	Dunes
82	8.16	0.64	0.552	248	1.60	0.210	0.1377	90000	0.35	12.5	2.76	27.9	Dunes
51	8.11	0.62	0.537	236	1.62	0.202	0.1243	68000	0.36	12.9	2.87	28.7	Dunes
52	8.01	0.55	0.497	222	1.81	0.188	0.0863	75300	0.43	14.1	3.08	31.0	Dunes
73	8.20	0.61	0.53	222	1.67	0.195	0.109	83600	0.38	13.1	2.97	29.1	Dunes
74	8.18	0.65	0.56	215	1.58	0.197	0.1242	84200	0.35	12.3	2.94	27.5	Dunes
76	8.49	0.63	0.544	203	1.69	0.188	0.0980	85000	0.38	12.7	3.08	28.3	Dunes
75	8.24	0.64	0.552	204	1.60	0.190	0.113	84000	0.35	12.5	3.05	27.9	Dunes
53	8.01	0.57	0.50	235	1.77	0.195	0.097	76300	0.41	14.0	2.97	30.8	Dunes
77	8.76	0.65	0.56	199	1.68	0.189	0.1012	84800	0.37	12.3	3.07	27.5	Dunes
96	8.31	0.53	0.468	201	1.94	0.174	0.0643	81000	0.47	15.1	3.33	32.9	Dunes
94	11.30	0.81	0.672	237	1.74	0.206	0.1120	91500	0.34	9.9	2.81	22.9	Dunes
83	15.58	0.91	0.74	200	2.14	0.218	0.0913	133000	0.40	8.8	2.66	20.8	Dunes
54	15.36	0.92	0.747	240	2.08	0.241	0.1072	132000	0.38	8.7	2.40	20.6	Dunes
56	15.36	0.90	0.733	242	2.14	0.239	0.0997	152000	0.40	8.9	2.42	21.0	Dunes
55	15.36	0.94	0.762	237	2.04	0.242	0.1125	110000	0.37	8.5	2.39	20.2	Dunes

(1) E. cont'd.

Run No.	Q cfs	D ft	R ft	S $\times 10^5$	V fps	V_τ fps	f	R	F	B/D	V_t/V_τ	d_s/R $\times 10^4$	Bed Form
57	15.39	0.87	0.714	259	2.20	0.244	0.0984	149500	0.42	9.2	2.37	21.6	Dunes
58	15.28	0.90	0.733	233	2.11	0.235	0.0993	143000	0.39	8.9	2.47	21.0	Dunes
95	15.38	0.80	0.667	180	2.39	0.196	0.0538	141700	0.47	10	2.96	23.1	Dunes
78	11.52	0.72	0.611	320	2.00	0.250	0.1250	114000	0.42	11.1	2.32	25.2	Dunes
59	15.36	0.65	0.56	326	2.96	0.242	0.0534	159300	0.65	12.3	2.39	27.5	Transition
60	21.35	0.62	0.537	342	4.28	0.213	0.0294	217000	0.96	12.9	2.38	28.7	Plane
61	21.32	0.61	0.53	355	4.36	0.246	0.0255	231500	0.98	13.1	2.35	29.1	Plane
71	8.22	0.32	0.296	531	3.21	0.225	0.0393	91200	1.00	25	2.57	52.0	Plane
72	8.26	0.32	0.296	550	3.26	0.229	0.0395	89200	1.02	25	2.53	52.0	Plane
70	8.14	0.30	0.279	640	3.41	0.240	0.0395	88000	1.10	26.7	2.52	55.2	Plane
63	15.50	0.43	0.388	570	4.48	0.267	0.0284	165500	1.20	18.6	2.17	39.7	Antidune
64	15.61	0.41	0.372	578	4.76	0.263	0.0244	168500	1.31	19.5	2.20	41.4	Antidune
65	15.60	0.42	0.381	571	4.63	0.265	0.0262	169300	1.26	19.0	2.19	40.4	Antidune
66	15.52	0.45	0.404	575	4.34	0.274	0.0318	173600	1.14	17.8	2.11	38.1	Antidune
80	15.27	0.39	0.355	643	4.91	0.271	0.0243	176600	1.39	20.5	2.14	43.4	Antidune
81	21.35	0.55	0.497	634	4.85	0.323	0.0354	184200	1.15	14.1	1.79	31.0	Standing Wave
62	21.23	0.54	0.476	622	4.89	0.309	0.0319	237500	1.17	14.8	1.87	32.4	Standing Wave
67	20.87	0.53	0.468	646	4.91	0.312	0.0323	225100	1.19	15.1	1.86	32.9	Standing Wave
79	21.31	0.55	0.484	651	4.82	0.319	0.035	222500	1.15	14.5	1.82	31.8	Standing Wave

(1) E. cont'd.

Run No.	Q cfs	D ft	R ft	S $\times 10^5$	V fps	V_τ fps	f	R	F	B/D	V_t/V_τ	d_s/R $\times 10^4$	Bed Form
84	15.36	0.41	0.372	740	4.67	0.298	0.0326	141000	1.29	19.5	1.94	54.4	Antidune
69	15.54	0.43	0.388	734	4.48	0.303	0.0366	170700	1.20	18.6	1.91	39.7	Antidune
98	15.80	0.44	0.396	821	4.51	0.324	0.0412	161300	1.20	18.2	1.79	38.9	Antidune
68	20.94	0.53	0.468	740	4.95	0.334	0.0364	232000	1.20	15.1	1.73	32.9	Standing Wave
100	21.42	0.51	0.452	790	5.28	0.339	0.033	184000	1.30	15.7	1.71	34.1	Plane
99	21.27	0.50	0.444	806	5.32	0.339	0.0324	216800	1.33	16	1.71	34.7	Antidune
97	12.01	0.37	0.339	960	4.07	0.323	0.0504	127100	1.18	21.6	1.79	45.4	Antidune

F. d_s = 0.93 mm V_t = 2.27 fps

Run No.	Q cfs	D ft	R ft	S $\times 10^5$	V fps	V_T fps	f	R	F	B/D	V_t/V	d_s/R $\times 10^4$	Bed Form
19	8.06	1.01	0.808	13	1.00	0.058	0.0269	74000	0.18	7.9	39.1	37.8	Plane
25	9.88	1.01	0.808	22	1.22	0.076	0.031	89500	0.21	7.9	29.8	37.8	Plane
26	10.80	1.02	0.817	22	1.32	0.075	0.0258	96000	0.23	7.8	30.2	37.3	Plane
27	11.86	1.01	0.808	28	1.47	0.085	0.0267	116500	0.26	7.9	26.7	37.8	Plane
20	10.91	1.03	0.817	28	1.32	0.086	0.034	99500	0.23	7.8	26.3	37.3	Plane
21	12.06	1.01	0.808	30	1.49	0.088	0.0279	112500	0.26	7.9	25.9	37.8	Plane
18	13.42	1.01	0.808	37	1.66	0.098	0.0279	117500	0.29	7.9	23.1	37.8	Dune
28	14.53	1.04	0.825	37	1.75	0.099	0.0256	136500	0.30	7.7	23.0	37.0	Dune
29	4.62	0.50	0.444	43	1.16	0.077	0.0352	46500	0.29	16	29.4	68.7	Plane
22	4.49	0.49	0.438	43	1.15	0.078	0.0368	45300	0.29	16.3	29.3	69.6	Plane

(1) F . cont'd.

Run No.	Q cfs	D ft	R ft	S $\times 10^5$	V fps	V_τ fps	f	R	F	B/D	V_t/V_τ	d_s/R $\times 10^4$	Bed Form
30	5.06	0.51	0.452	50	1.25	0.085	0.0370	51000	0.31	15.7	26.8	67.5	Plane
31	5.42	0.50	0.444	54	1.36	0.088	0.0335	51200	0.34	16	25.9	68.7	Plane
15	16.25	1.05	0.833	59	1.93	0.126	0.0341	147500	0.33	7.6	18.1	36.6	Dune
23	5.10	0.49	0.438	62	1.30	0.093	0.0409	51700	0.33	16.3	24.5	69.6	Plane
32	6.25	0.52	0.46	64	1.50	0.097	0.0335	58500	0.37	15.4	23.4	66.3	Plane
24	5.71	0.49	0.438	68	1.46	0.098	0.0360	58100	0.37	16.3	23.1	69.6	Plane
14	7.41	0.58	0.507	71	1.60	0.108	0.0364	70000	0.37	13.8	21.1	60.2	Dune
34	7.08	0.54	0.476	80	1.64	0.111	0.0366	70800	0.39	14.8	20.5	64.1	Dune
16	16.85	1.04	0.825	112	2.03	0.173	0.058	152000	0.35	7.7	13.1	37.0	Dune
35	7.64	0.53	0.497	130	1.80	0.144	0.0513	76400	0.44	15.1	15.7	61.4	Dune
17	16.83	1.00	0.80	136	2.10	0.187	0.0635	152800	0.37	8.0	12.2	38.2	Dune
33	8.18	0.56	0.491	145	1.83	0.152	0.0552	81000	0.43	14.3	15.0	62.1	Dune
5	16.41	0.93	0.755	183	2.21	0.211	0.0730	144000	0.40	8.6	10.8	40.4	Dune
10	6.90	0.46	0.412	192	1.88	0.160	0.0578	69800	0.49	17.4	14.2	74.0	Dune
37	22.58	1.11	0.869	275	2.54	0.277	0.095	194000	0.43	7.2	8.2	35.1	Dune
36	8 96	0.55	0.482	304	2.04	0.217	0.0905	84700	0.48	14.6	10.5	63.3	Dune
6	22.30	1.04	0.825	313	2.68	0.289	0.0930	20000	0.46	7.7	7.87	37.0	Dune
7	10.10	0.59	0.513	339	2.14	0.237	0.098	97000	0.49	18.6	1.00	59.5	Dune
38	22.69	1.02	0.817	356	2.78	0.306	0.0968	205000	0.49	7.8	7.43	37.3	Dune

(1) F. cont'd.

Run No.	Q cfs	D ft	R ft	S $\times 10^5$	V fps	V_τ fps	f	IR	IF	B/D	V_t/V_τ	d_s/R $\times 10^4$	Bed Form
11	22.22	0.92	0.747	393	3.02	0.307	0.0826	200000	0.56	8.7	7.40	40.8	Dune
8	11.20	0.57	0.50	430	2.46	0.263	0.0915	106000	0.57	14.0	8.63	61.0	Dune
12	22.19	0.89	0.727	437	3.12	0.320	0.0842	224000	0.58	9.0	7.10	42.0	Dune
13	22.09	0.82	0.678	587	3.37	0.359	0.0907	202000	0.65	9.8	6.32	45.0	Transition
9	11.32	0.49	0.437	600	2.89	0.291	0.0812	113000	0.72	16.3	7.80	69.8	Transition
3	16.46	0.60	0.523	650	3.43	0.331	0.0745	155000	0.78	13.3	6.87	58.3	Transition
1	22.33	0.68	0.584	710	4.10	0.365	0.0635	217500	0.88	11.7	6.23	52.2	Transition
2	22.07	0.53	0.468	920	5.20	0.372	0.0409	215000	1.26	15.1	6.10	65.2	Transition
4	15.64	0.51	0.452	940	3.83	0.369	0.0742	151500	0.95	15.7	6.15	67.5	Transition
41	15.67	0.44	0.396	1120	4.45	0.378	0.0577	169500	1.18	18.2	6.00	77.0	Transition
42	20.44	0.44	0.396	1160	5.81	0.384	0.0349	215000	1.54	18.2	5.9	77.0	Standing Wave
40	15.53	0.38	0.246	1230	5.11	0.312	0.0298	115200	1.46	21.1	7.28	124.0	Standing Wave
43	20.63	0.44	0.396	1260	5.86	0.402	0.0376	221500	1.56	18.2	5.66	77.0	Standing Wave
39	20.88	0.43	0.388	1280	6.07	0.399	0.0346	220000	1.63	18.6	5.70	78.6	Standing Wave

(2) Barton and Lin(4), 4-ft flume

d_s = 0.18 mm V_t = 0.085 fps

Run No.	Q cfs	D ft	R ft	S $x10^5$	V fps	V_τ fps	f	R	F	B/D	V_t/V_τ	d_s/R $x10^4$	Bed Form
13	1.53	0.54	0.425	45	0.71	0.0785	0.099	25000	0.216	7.41	1.08	13.9	Dunes
12	1.96	0.66	0.496	44	0.74	0.084	0.103	30400	0.202	6.07	1.01	11.9	Dunes
21	0.90	0.30	0.261	160	0.75	0.116	0.192	16200	0.277	13.33	0.733	22.6	Dunes
11	1.5	0.46	0.374	87	0,815	0.102	0.126	35200	0.257	8.7	0.832	15.8	Dunes
17	1.34	0.36	0.305	161	0.93	0.126	0.147	23400	0.235	11.1	0.674	19.3	Dunes
10	2.0	0.51	0.406	88	0.98	0.107	0.096	32900	0.282	7.85	0.794	14.5	Dunes
16	1.90	0.40	0.333	158	1.19	0.130	0.095	32700	0.365	10	0.654	17.7	Dunes
8	3.1	0.65	0.490	81	1.19	0.115	0.0735	48200	0.291	6.16	0.739	12.0	Dunes
27	2.1	0.40	0.333	135	1.31	0.122	0.070	32800	0.367	10	0.697	17.7	Dunes
3	3.0	0.56	0.438	86	1.34	0.110	0.054	48500	0.320	7.15	0.772	13.5	Dunes
28	2.64	0.48	0.387	116	1.39	0.120	0.059	44500	0.390	8.34	0.708	15.3	Dunes
5	3.5	0.63	0.479	866	1.39	0.115	0.055	55000	0.347	6.35	0.739	12.3	Dunes
32	4.15	0.73	0.535	82	1.42	0.119	0.056	62800	0.323	5.48	0.714	11.0	Dunes
1	4.45	0.78	0.561	88	1.43	0.126	0.060	66300	0.300	5.13	0.674	10.5	Dunes
6	4.0	0.69	0.513	88	1.45	0.121	0.056	61500	0.327	5.8	0.702	11.5	Dunes
15	2.70	0.45	0.368	150	1.50	0.133	0.063	45700	0.430	8.9	0.638	16.0	Dunes
30	5.8	0.94	0.640	555	1.54	0.107	0.038	81500	0.290	4.26	0.794	9.2	Dunes
34	8.85	1.38	0.816	65	1.60	0.131	0.054	108000	0.249	2.9	0.648	7.2	Dunes
7	5.5	0.84	0.591	88	1.64	0.130	0.050	80000	0.344	4.77	0.654	10.0	Dunes

(2) cont'd.

Run No.	Q cfs	D ft	R ft	S $\times 10^5$	V fps	V_τ fps	f	R	F	B/D	V_t/V_τ	d_s/R $\times 10^4$	Bed Form
33	7.2	1.03	0.673	61	1.75	0.115	0.0346	97400	0.283	3.88	0.739	8.8	Dunes to Sand Bar
29	5.8	0.60	0.461	121	2.41	0.134	0.0248	91700	0.573	6.67	0.634	12.8	Flat
31	4.2	0.41	0.340	123	2.56	0.116	0.0164	72000	0.738	9.8	0.733	17.4	Flat
26	7.1	0.69	0.513	125	2.58	0.144	0.025	109000	0.575	5.8	0.59	11.5	Flat
25	8.1	0.78	0.561	124	2.60	0.150	0.0266	121000	0.553	5.1	0.667	10.5	Flat
18	7.40	0.69	0.513	156	2.68	0.161	0.029	114000	0.603	5.8	0.528	11.5	Flat
20	6.7	0.61	0.467	166	2.74	0.158	0.0266	105500	0.670	6.6	0.538	12.6	Flat
23	7.4	0.65	0.490	183	2.84	0.170	0.0288	115000	0.695	6.2	0.5	12.0	Flat
22	9.1	0.76	0.586	170	2.99	0.179	0.0287	145000	0.661	5.3	0.474	10.1	Flat
19	9.0	0.75	0.545	167	3.00	0.171	0.026	135000	0.644	5.3	0.497	10.8	Flat
35	7.2	0.56	0.437	160	3.22	0.150	0.0173	116000	0.786	7.1	0.567	13.5	Flat
36	7.6	0.53	0.419	210	3.60	0.168	0.0174	125000	0.915	7.6	0.506	14.1	Flat

(3) CIT Experiments

A. Brooks (8) 0.875-ft flume

d_s = 0.16 mm V_t = 0.067 fps

Run No.	Q cfs	D ft	R ft	S $\times 10^5$	V fps	V_τ fps	f	R	F	B/D	V_t/V_τ	d_s/R $\times 10^4$	Bed Form
2	0.54	0.284	0.172	180	2.15	0.100	0.017	30600	0.71	3.08	0.673	30 5	Smooth
3	0.435	0.243	0.156	250	2.04	0.112	0.024	26300	0.73	3.60	0.600	33.7	Smooth
4	0.43	0.236	0.153	240	2.08	0.108	0.022	26300	0.75	3.71	0.623	34.3	Smooth
5	0.28	0.18	0.13	310	1.8	0.115	0.033	19300	0.74	4.86	0.584	40.4	Meanders
6	0.345	0.195	0.135	240	2.00	0.103	0.021	22300	0.80	4.48	0.653	38.9	Smooth
7	0.435	0.243	0.156	210	2.04	0.103	0.020	26300	0.73	3.60	0.653	33.7	Smooth
8	0.375	0.24	0.155	230	1.75	0.11	0.030	22400	0.63	3.65	0.611	33.9	Meanders
9	0.285	0.245	0.155	260	1.35	0.115	0.059	17300	0.47	3.57	0.585	33.9	Dunes
10	0.20	0.25	0.16	200	0.93	0.10	0.095	12300	0.33	3.50	0.673	32.8	Dunes
11	0.205	0.155	0.115	330	1.5	0.11	0.043	14250	0.67	5.65	0.611	45.7	Meanders
12	0.37	0.30	0.178	220	1.40	0.111	0.050	10600	0.45	2.92	0.606	29.5	Dunes
13	0.215	0.197	0.136	350	1.25	0.124	0.078	14050	0.50	4.44	0.542	38.6	Dunes

(3) cont'd.

B. Brooks and Vanoni (8) 2.79-ft flume, $d_s = 0.137$, $V_t = 0.049$ fps

Run No.	Q cfs	D ft	R ft	S $\times 10^5$	V fps	V_τ fps	f	R	F	B/D	V_t/V_τ	d_s/R $\times 10^4$	Bed Form
2-9	0.510	0.238	0.203	141	0.77	0.096	0.124	12900	0.28	11.7	0.51	22.1	Dunes
2-3	0.615	0.243	0.207	204	0.90	0.117	0.133	15400	0.32	11.5	0.42	21.7	Dunes
2-8	0.715	0.240	0.205	280	1.07	0.136	0.129	18100	0.38	11.6	0.36	21.9	Dunes
2-1	0.855	0.240	0.205	278	1.28	0.135	0.090	21700	0.46	11.6	0.36	21.9	Dunes
2-7	0.930	0.237	0.203	277	1.40	0.134	0.074	23500	0.51	11.8	0.37	22.1	Dunes
2-6	1.00	0.249	0.211	246	1.44	0.129	0.064	25100	0.51	11.2	0.38	21.3	Dunes
2-17D[a]	1.17	0.302	0.248	201	1.39	0.127	0.067	28500	0.44	9.24	0.39	18.1	Dunes
2-17F[b]	1.17	0.203	0.177	276	2.07	0.125	0.029	30300	0.81	13.75	0.39	25.4	Flat
2-2	1.38	0.233	0.200	205	2.13	0.115	0.0235	35200	0.78	12.00	0.43	22.5	Flat
2-12	1.21	0.541	0.390	39	0.80	0.070	0.061	25800	0.19	5.17	0.70	11.5	Dunes
2-5	1.54	0.528	0.383	70	1.04	0.092	0.063	32900	0.25	5.28	0.53	11.7	Dunes
2-10	1.87	0.549	0.394	105	1.22	0.116	0.072	39700	0.29	5.09	0.42	11.4	Dunes
2-11	2.23	0.536	0.387	122	1.49	0.123	0.055	47800	0.36	5.21	0.40	11.6	Dunes
2-13D[a]	2.65	0.553	0.396	102	1.72	0.119	0.038	56300	0.41	5.05	0.41	11.3	Dunes
2-16F[b]	3.50	0.524	0.381	107	2.39	0.115	0.0185	75200	0.59	5.33	0.43	11.8	Flat
2-4	3.84	0.544	0.391	107	2.53	0.116	0.0170	81700	0.60	5.13	0.42	11.5	Flat

[a] Dune section of flow with a long sand wave

[b] Flat section of flow with a long sand wave

(3) cont'd.

C. Kennedy (23) 0.875-ft flume
d_s = 0.549 mm V_t = 1.00 fps

Run No.	Q cfs	D ft	R ft	S $\times 10^5$	V fps	V_τ fps	f	R	F	B/D	V_t/V_τ	d_s/R $\times 10^4$	Bed Form
5-11	0.200	0.074	0.0632	2080	3.09	0.206	0.0356	16100	2.00	11.8	5.43	285	
5-12	0.246	0.084	0.0705	2140	3.35	0.221	0.0348	19500	2.04	10.4	4.97	255	
5-13	0.257	0.092	0.0762	1850	3.20	0.213	0.0354	20200	1.86	9.52	4.68	236	
5-18	0.256	0.093	0.0765	1820	3.15	0.212	0.0362	19900	1.82	9.41	4.71	235	
5-14	0.500	0.123	0.0960	2720	4.65	0.292	0.0315	36900	2.34	7.11	3.43	188	
5-2	0.214	0.148	0.110	560	1.65	0.141	0.0585	15000	0.75	5.91	7.10	164	
5-10	0.287	0.150	0.112	810	2.19	0.171	0.0486	20300	1.00	5.83	5.95	161	
5-7	0.334	0.147	0.110	1090	2.60	0.196	0.0456	23600	1.19	5.95	5.10	164	
5-4	0.360	0.150	0.111	1250	2.74	0.211	0.0474	25100	1.25	5.83	5.07	162	
5-9	0.463	0.159	0.116	1400	3.33	0.229	0.0378	31900	1.47	5.50	4.84	155	
5-16	0.465	0.154	0.114	1340	3.45	0.222	0.0331	32500	1.55	5.68	5.40	158	
5-17	0.455	0.146	0.110	1540	3.56	0.233	0.0343	32400	1.64	6.00	4.97	164	
5-8	0.550	0.147	0.110	1870	4.27	0.257	0.0291	38800	1.96	5.95	4.51	164	
5-3	0.468	0.245	0.157	550	2.18	0.167	0.0470	28300	0.77	3.57	19.1	115	
5-5	0.742	0.239	0.155	1100	3.55	0.234	0.0348	4550	1.28	3.66	9.1	116	
5-1	0.782	0.346	0.193	670	2.58	0.204	0.0500	40200	0.77	2.53	15.0	93.3	

(3) cont'd.

D. Kennedy (23) 2.79-ft flume
d_s = 0.233 mm V_t = 0.181 fps

Run No.	Q cfs	D ft	R ft	S $\times 10^5$	V fps	V_τ fps	f	IR	IF	B/D	V_t/V_τ	d_s/R $\times 10^4$	Bed Form
4-25	0.215	0.157	0.115	320	1.57	0.109	0.0386	14900	0.70	5.57	0.89	66.5	
4-37	0.265	0.151	0.112	380	2.01	0.117	0.0272	18600	0.91	5.80	1.34	68.3	
4-24	0.290	0.147	0.110	480	2.26	0.130	0.0266	20900	1.04	5.95	1.04	69.6	
4-29	0.332	0.154	0.114	730	2.46	0.164	0.0354	23200	1.10	5.68	0.90	67.1	
4-28	0.330	0.148	0.111	660	2.55	0.152	0.0289	23400	1.17	5.91	1.15	68.9	
4-26	0.359	0.153	0.113	950	2.68	0.186	0.0386	25000	1.21	5.72	0.84	67.7	
4-27	0.438	0.152	0.113	1600	3.29	0.241	0.0429	30700	1.49	5.76	0.46	67.7	
4-1	0.434	0.236	0.153	260	2.10	0.113	0.0233	26600	0.76	3.71	1.09	50.0	
4-30	0.468	0.251	0.160	260	2.13	0.115	0.0235	26900	0.75	3.49	1.00	47.8	
4-31	0.620	0.256	0.162	420	2.77	0.148	0.0227	37100	0.96	3.42	1.12	47.2	
4-36	0.622	0.247	0.158	450	2.88	0.151	0.0221	37600	1.02	3.52	1.03	48.4	
4-33	0.716	0.248	0.158	650	3.30	0.182	0.0244	43100	1.17	3.53	0.65	48.4	
4-32	0.775	0.259	0.163	940	3.42	0.222	0.0337	46100	1.18	3.38	0.50	46.9	
4-38	0.772	0.346	0.193	260	2.55	0.127	0.0199	40700	0.76	2.53	0.94	39.6	
4-12	0.683	0.145	0.131	340	1.69	0.120	0.0401	18300	0.78	19.25	1.51	58.4	
4-10	0.898	0.154	0.139	420	2.09	0.137	0.0346	24000	0.94	18.1	1.32	55.0	
4-22	1.086	0.148	0.134	680	2.63	0.171	0.0338	29100	1.18	18.85	0.89	57.1	

(3) D. cont'd.

Run No.	Q cfs	D	R	S $\times 10^5$	V fps	V_τ fps	f	IR	IF	B/D	V_t/V_τ	d_s/R $\times 10^4$	Bed Form
4-11	1.131	0.148	0.134	820	2.74	0.188	0.0377	30300	1.26	18.85	0.61	57.1	
4-7	1.71	0.195	0.171	880	3.14	0.220	0.0393	44300	1.25	14.3	0.45	44.7	
4-6	2.00	0.218	0.188	2290	3.29	0.372	0.102	51200	1.24	12.8	0.28	40.7	
4-3	0.86	0.228	0.196	260	1.35	0.128	0.0709	21900	0.50	12.23	0.47	39.0	
4-19	1.50	0.252	0.214	210	2.13	0.120	0.0255	34500	0.75	11.08	0.62	35.8	
4-17	1.96	0.253	0.214	340	2.77	0.152	0.0242	49000	0.97	11.02	0.64	35.8	
4-16	2.48	0.257	0.217	710	3.45	0.223	0.0335	61800	1.20	10.85	0.39	35.3	
4-13	2.45	0.335	0.270	250	2.62	0.148	0.0254	58400	0.89	8.32	0.71	28.3	
4-23	2.467	0.356	0.284	170	2.48	0.124	0.0202	58200	0.73	7.83	0.68	26.9	
4-14	3.32	0.348	0.279	320	3.42	0.170	0.0197	78900	1.02	8.00	0.53	27.4	

E. Kennedy (24) 2.79-ft flume

d_s = 0.142 mm V_t = 0.053 fps

Run No.	Q cfs	D ft	R ft	S $\times 10^5$	V fps	V_τ fps	f	IR	IF	B/D	V_t/V_τ	d_s/R $\times 10^4$	Bed Form
3-1	1.395	0.550	0.395	56	0.91	0.084	0.068	29700	0.22	5.08	0.631	11.8	Dunes
3-4	1.403	0.441	0.335	145	1.14	0.125	0.096	31600	0.30	6.33	0.424	13.9	Dunes
3-2	1.045	0.373	0.294	206	1.35	0.140	0.086	32800	0.39	7.49	0.378	15.9	Dunes
3-7	1.395	0.345	0.277	198	1.45	0.133	0.067	33200	0.44	8.09	0.398	16.8	Dunes
3-5D	1.395	0.340	0.273	160	1.47	0.119	0.052	33200	0.44	8.21	0.445	17.1	Dunes (S.W.)

(3) E. cont'd.

Run No.	Q cfs	D ft	R ft	S $\times 10^5$	V fps	V_τ fps	f	IR	IF	B/D	V_t/V_τ	d_s/R $\times 10^4$	Bed Form
3-5F	1.395	0.254	0.215	250	1.97	0.131	0.036	35000	0.69	11.00	0.404	21.7	Flat(S.W.)
3-6[a]	1.397	0.235	0.201	198	2.13	0.113	0.023	35400	0.78	11.90	0.469	23.2	Flat
3-6	1.397	0.233	0.200	207	2.15	0.115	0.023	35500	0.78	12.00	0.461	23.3	Flat
3-6[b]	1.045	0.228	0.196	221	2.21	0.118	0.023	35800	0.82	12.25	0.449	23.8	Flat

F. Vanoni and Hwang (47) 3.61-ft flume
d_s = 0.206 mm V_t = 0.111 fps

Run No.	Q cfs	D ft	R ft	S $\times 10^5$	V fps	V_τ fps	f	IR	IF	B/D	V_t/V_τ	d_s/R $\times 10^4$	Bed Form
1	2.26	0.598	0.449	64	1.05	0.096	0.068	38900	0.24	6.0	1.157	15.1	
2	3.09	0.589	0.444	105	1.45	0.123	0.057	53300	0.33	6.1	0.907	15.2	
3	3.82	0.578	0.438	130	1.83	0.136	0.044	66200	0.42	6.3	0.822	15.4	
4	3.22	0.589	0.444	111	1.51	0.126	0.056	55600	0.35	6.1	0.882	15.2	
5	3.37	0.603	0.452	110	1.55	0.127	0.053	57800	0.35	6.0	0.881	15.0	
8	2.30	0.591	0.445	71	1.08	0.101	0.070	39700	0.25	6.1	1.105	15.2	

(4) Stein (44) 4-ft flume
d_s = 0.4 mm

Run No.	Q cfs	D ft	R ft	S $\times 10^5$	V fps	V_τ fps	f	R	F	B/D	V_t/V_τ	d_s/R $\times 10^4$	Bed Form
2	5.36	0.600	0.462	352	2.233	0.229	0.084	85000	0.51	6.7	1.83	28.4	
4	4.05	0.60	0.462	285	1.687	0.206	0.119	64400	0.38	6.7	2.04	28.4	
5	7.06	0.60	0.462	321	2.942	0.218	0.044	112000	0.67	6.7	1.92	28.4	
6	8.49	0.60	0.462	331	3.538	0.222	0.031	135000	0.80	6.7	1.89	28.4	
7	10.03	0.60	0.462	508	4.179	0.275	0.035	159000	0.95	6.7	1.52	28.4	
8	11.60	0.60	0.462	736	4.833	0.331	0.037	184000	1.10	6.7	1.27	28.4	
9	13.00	0.60	0.462	1079	5.417	0.400	0.044	207000	1.23	6.7	1.05	28.4	
22	5.52	0.80	0.571	201	1.725	0.192	0.099	81500	0.34	5.0	2.18	23.0	
23	7.01	0.80	0.571	298	2.191	0.234	0.091	103000	0.43	5.0	1.79	23.0	
24	8.51	0.80	0.571	297	2.659	0.234	0.062	126000	0.52	5.0	1.79	23.0	
25	9.99	0.80	0.571	285	3.122	0.229	0.043	147000	0.62	5.0	1.83	23.0	
26	11.50	0.80	0.571	269	3.594	0.222	0.031	170000	0.71	5.0	1.88	23.0	
27	13.00	0.80	0.571	261	4.063	0.219	0.023	192000	0.80	5.0	1.91	23.0	
28	14.50	0.81	0.577	327	4.475	0.246	0.024	213000	0.88	4.9	1.70	22.7	
29	16.00	0.80	0.571	417	5.000	0.277	0.025	236000	0.99	5.0	1.51	23.0	
30	17.00	0.81	0.577	524	5.247	0.312	0.028	250000	1.03	4.9	1.34	22.7	
31	10.70	0.80	0.571	286	3.344	0.229	0.038	158000	0.66	5.0	1.83	23.0	
32	9.32	0.81	0.577	249	2.877	0.215	0.045	137000	0.56	4.9	1.95	22.7	

(4) cont'd.

Run No.	Q cfs	D ft	R ft	S $\times 10^5$	V fps	V_τ fps	f	IR	IF	B/D	V_t/V_τ	d_s/R $\times 10^4$	Bed Form
33	6.28	0.80	0.571	267	1.962	0.222	0.102	92700	0.39	5.0	1.89	23.0	
34	2.98	0.40	0.333	347	1.863	0.193	0.086	51300	0.52	10.0	2.17	39.3	
35	4.05	0.41	0.340	387	2.470	0.206	0.056	69400	0.68	9.8	2.03	38.5	
36	4.97	0.40	0.333	370	3.106	0.199	0.033	85600	0.87	10.0	2.10	39.3	
37	5.40	0.40	0.333	427	3.738	0.214	0.026	103000	1.04	10.0	1.96	39.3	
38	7.07	0.40	0.333	661	4.419	0.266	0.029	122000	1.23	10.0	1.57	39.3	
39	7.99	0.40	0.333	101	4.994	0.104	0.003	138000	1.39	10.0	4.02	39.3	
40	8.99	0.40	0.333	130	5.619	0.118	0.004	155000	1.57	10.0	3.54	39.3	
41	9.91	0.41	0.340	169	6.043	0.136	0.004	170000	1.66	9.8	3.07	38.5	
45	6.42	0.69	0.513	348	2.326	0.240	0.085	98600	0.49	5.8	1.75	25.5	
46	5.52	0.59	0.456	395	2.339	0.241	0.085	88100	0.54	6.8	1.74	28.7	
47	4.61	0.50	0.400	387	2.305	0.223	0.075	76200	0.57	8.0	1.88	32.8	
48	2.76	0.30	0.261	403	2.300	0.184	0.051	49600	0.74	13.3	2.28	50.2	
49	13.90	0.70	0.519	553	4.964	0.304	0.030	213000	1.05	5.7	1.38	25.2	
50	11.10	0.60	0.462	524	4.625	0.279	0.029	176000	1.05	6.7	1.50	28.4	
51	3.93	0.32	0.276	398	3.070	0.188	0.030	70000	0.96	12.5	2.23	47.5	
52	8.42	0.49	0.394	529	4.296	0.259	0.029	140000	1.08	8.2	1.62	33.3	
53	4.72	0.30	0.261	491	3.933	0.203	0.021	84800	1.27	13.3	2.06	50.2	
54	9.97	0.49	0.394	980	5.087	0.352	0.038	165000	1.28	8.2	1.19	33.3	
55	9.24	0.49	0.394	679	4.714	0.293	0.031	153000	1.19	8.2	1.43	33.3	

(4) cont'd.

Run No.	Q cfs	D ft	R ft	S $\times 10^5$	V fps	V_τ fps	f	R	F	B/D	V_t/V_τ	d_s/R $\times 10^4$	Bed Form
56	15.20	0.69	0.513	705	5.507	0.341	0.031	233000	1.17	5.8	1.23	25.5	
57	12.60	0.71	0.524	365	4.437	0.248	0.025	192000	0.93	5.6	1.69	25.0	
58	11.30	0.71	0.524	304	3.979	0.226	0.026	172000	0.83	5.6	1.85	25.0	
107	5.00	0.60	0.462	352	2.083	0.229	0.096	79500	0.47	6.7	1.83	28.4	
108	4.00	0.60	0.462	294	1.667	0.209	0.126	63600	0.38	6.7	2.00	28.4	
109	3.60	0.60	0.462	225	1.500	0.183	0.119	57200	0.34	6.7	2.29	28.4	
110	6.00	0.60	0.462	318	2.500	0.217	0.060	95400	0.57	6.7	1.93	28.4	
111	6.60	0.60	0.462	328	2.750	0.221	0.052	105000	0.63	6.7	1.90	28.4	
112	7.10	0.60	0.462	332	2.958	0.222	0.045	113000	0.67	6.7	1.89	28.4	
113	5.50	0.60	0.462	320	2.292	0.218	0.072	87400	0.52	6.7	1.92	28.4	
114	4.50	0.60	0.462	331	1.875	0.222	0.112	71500	0.43	6.7	1.89	28.4	
115	1.80	0.30	0.261	212	1.500	0.133	0.063	32300	0.48	13.3	3.14	50.2	
116	2.00	0.30	0.261	306	1.667	0.160	0.074	35900	0.54	13.3	2.61	50.2	